DISSERTATION

on

Inverse Vehicle Dynamic Model of A Bicycle Vehicle with Power Steering: A Bond Graph Approach

Submitted in partial fulfilment of the requirement for the award of degree of

Master of Engineering

IN

CAD/CAM Engineering

Submitted By

Anshuman

Roll No. 801281005

Under the Supervision of

Dr. Tarun Kumar Bera

Assistant Professor
Department of Mechanical Engineering
Thapar University,
Patiala

DEPARTMENT OF MECHANICAL ENGINEERING
THAPAR UNIVERSITY
PATIALA-147004, INDIA

JULY 2014

This thesis is dedicated to

my parents

DECLARATION

I hereby declare that the seminar report entitled **"Inverse Vehicle Dynamic Model of a Bicycle Vehicle With Power Steering: A Bond Graph Approach"** in the partial fulfilment for award of degree of **Master of Engineering** submitted in **Department of Mechanical Engineering, Thapar University, Patiala,** is a record of my own work carried out under the supervision and guidance of **Dr. T. K. Bera, Department of Mechanical Engineering, Thapar University.** This matter embodied in this report has not been submitted in part or full to any other university or institute for the award of any degree.

(Anshuman)

This is to certify that above declaration made by the student concerned is correct to the best of my knowledge & belief.

Dr. Tarun Kumar Bera
Assistant Professor
Thapar University, Patiala

Countersigned by:

Head of ME Department
Thapar University, Patiala

Dean of Academic Affairs
Thapar University, Patiala

ACKNOWLEDGEMENT

Every endeavour in itself is an impression of the efforts of not only those who pursue it but of those as well who provide guidance and motivation towards its successful completion. Likewise, this thesis bears an imprint of all those who helped me at various stages and it would be unfair on my part not to thank them.

I express my sincere gratitude and thanks to my supervisor, **Dr. Tarun Kumar Bera**, Assistant Professor, department of mechanical engineering, Thapar University, Patiala, guide for his able guidance, continuous support and cooperation throughout my thesis , without which the present work would not have been possible. It was an honour and privilege to work under him as a student.

I am also grateful to Dr. Ajay Batish, Professor and Head, Mechanical Engineering Department for providing the facilities for the completion of the work.

Also, I am thankful to my family member and friends for their continued guidance and invaluable encouragement.

(Anshuman)

Roll No. 801281005

ABSTRACT

As the traffic is increasing day by day the possibility of accidents are increasing. These accidents are due to the human errors. Development of inverse dynamic controller necessary as it can replace the driver and track the predefined path. A bond graph model of a bicycle vehicle is developed and in this model manual and electrical power steering systems are attached and a comparison of both systems for evaluating the response is done. An inverse vehicle dynamics model is developed. This inverse model gives a torque to a bicycle model to follow a predefined path. An expression is derived to compute the steering angle in terms of longitudinal velocity and vehicle yaw rate for a predefine path. The inverse vehicle dynamics model is connected by an overwhelming controller in such a way that the output of forward model is feedback to inverse bicycle model. The vehicle's position is compared with the desired trajectory and the error signal is given to the inverse bicycle model to produce the desired output.

Keywords: Bicycle model, Bond graph modelling, Electrical power steering, Ghost controller, Inverse bicycle model, Manual steering, Overwhelming controller.

LIST OF ABBREVIATIONS

ABS	Antilock Braking System
ALVINN	Autonomous Land Vehicle In A Neural Network
C	Capacitance
CEPS	Column Assisted Electrical Power Steering
CG	Centre of Gravity
DARPA	Defence Advanced Research Project Agency
De	Effort Detector
Df	Flow Detector
DOF	Degree of Freedom
EPS	Electrical Power Steering
GY	Gyrator
HPS	Hybrid Power Steering
I	Inertia
ITB	Independent Axle Torque Biasing
LQR	Linear Quadratic Regulator
MSE	Modulated Source of Effort
MSF	Modulated Source of Flow
MTF	Modulated Transformer
MGY	Modulated Gyrator
PWS	Power Wheeled Steering
R	Resistance
REPS	Rack Assisted Power Steering
SBW	Steer by Wire
SE	Source of Effort
SF	Source of Flow
SR	Slip Ratio

NOMENCLATURE

K_{SW}	Steering Wheel Stiffness
J_{sw}	Steering Wheel Inertia
R_{sw}	Steering Wheel Damping Coefficient
L_i	Motor Coil Inductance
R_{co}	Motor Coil Resistance
R_{sh}	Motor Shaft Damping
μ_{mo}	Motor Constant
μ_h	Overwhelming High Gain
μ_l	Overwhelming Low Gain
V	Voltage
I	Motor Current
r_1	Steering Linkage ratio
r_2	Ball Screw Reduction Ratio
M	Mass of Bicycle Vehicle
K	Compliance Element
r_g	Reduction Gear Ratio
M_{ra}	Mass of Rack
M_i	Vartual Mass of Inverse Bicycle Vehicle Model
R_{ra}	Rack Damping Coefficient

LIST OF FIGURES

LIST OF TABLES

TABLE OF CONTENTS

CHAPTER 1 INTRODUCTION

Day by day numbers of vehicles on road are increasing by which roads are becoming congested and risky. 1.24 million people were perished on the world's roads in 2010 [**1**] and this is intolerably high. Some changes in the transportation control system are required. Most of the road accidents happen due to human errors. In mostly developed countries, transport infrastructure has been improved. The advanced freeways are ten times securer than regular roads but it is not economically favourable to establish new roads with intelligent traffic control systems. One of the options to encounter this problem is the entry of intelligent autonomous vehicle. An autonomous vehicle is described as the vehicle which can move on its own or the one which is self-driven. An intelligent vehicle is able to reduce 90% of road accidents that are caused by human error and can save human life [**2**].

1.1 BACKGROUND AND MOTIVATION

This section provides a history of the evolution of unmanned vehicles. Two hundred decades before, Hero of Alexandria designed a steer-by-wire robot which was able to act as a double lane change manoeuvre using feed-forward control. At that time, the fastest vehicles on the roads have been driven with the muscle power and guided by drivers. The high driving force maintained by houses or by the wind in that historical period [**3**].

100 decades after Hero, there had been small advancement in the direction of self-derived vehicles. A clockwork tricycle is invented by Leonardo da Vinci, a modern reconstruction of which is exhibited at Science History's Museum in Florence. The clockwork mechanism was based on spring, which stores energy and gives steering effort. In the early 1980s, first robot car was developed by Ernst Dickmanns. He introduced a vision system which provided the relevant input, but due to presence of noise the vision system results were uncertain. In 1987, his robot car with noise filter was able to run at higher speeds on empty streets [**4**].

In the year 1990, another innovator in autonomous vehicle field was Dean Pomerleau and he invented ALVINN (Autonomous Land Vehicle in a Neural Network). ALVINN was able to learn the path with some minutes training by a human driver [**5**]. In 1991, controller is proposed for analyzing the vehicle dynamics and a power wheeled steering method is used to steer the robotic car. The path is represented by straight lines and curves [**6**].

DARPA (Defence Advanced Research Projects Agency) started the first opulent Challenges in unmanned vehicle invention field. In 2004, DARPA offered one million dollar prize to the first unmanned vehicle able to cover a 150 mile track in Mojave Desert. The participating vehicles were GPS navigated with advanced computer technology. This competition was unsatisfactory as the best team covered only 7 miles. Later, DARPA re-organized competition and results were very impressive, five vehicles completed the 132 mile course. Stanford Racing Team guided by Sebastian Thrun won competition [**7**]. DARPA again organized a challenge in year 2007 in California urban environment but road were not open to public. The automated guided vehicles are also useful in many off road activities like assemble shop, hospitals, material storage.

In ordinary vehicle driver turns steering wheel and expects a particular yaw rate but vehicle does not response immediately or overshoot. Driver again turns steering wheel in reverse direction and tyres to get exact path. Power steering assist driver and provides better control on vehicle and enhance driver safety. Power steering allows driver to get the vehicle on desired path without requirement of high steering torque and increases the driver comfort. Power steering assists to judge the driving condition by some feedback. Inverse vehicle dynamics controller computes exact steering angle and torque to get exact path. It saves money in terms of fuel and time.

1.2 INVERSE VEHICLE DYNAMICS

Inverse vehicle dynamics is combination of inverse model of vehicle along with actual vehicle. Forward and inverse dynamic problem were first developed by Newton. The forward problem is to determine the kinematic parameters (position, velocity, acceleration) of body subjected to given set of forces. The inverse problem is to determine forces that should be applied to body to maintain the required kinematics parameters of the body in motion.

Fig. 1.1 Forward vehicle model

As shown in Fig. 1.1, input to the actual vehicle is steering angle and torque and the output is its centroid-position (x, y, θ). In the inverse model as shown in Fig. 1.2, the position is given as input; required torque and steering angle are determined using control law.

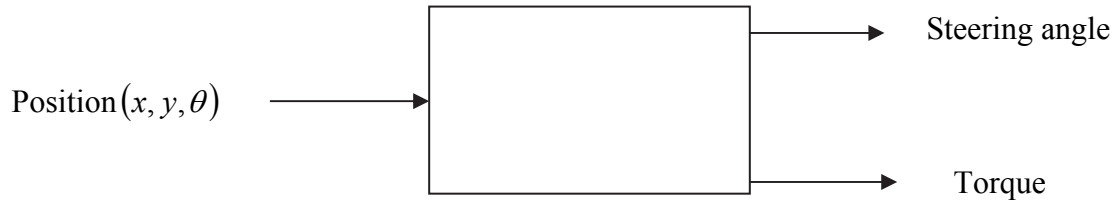

Fig. 1.2 Inverse vehicle model

The inverse approach is used in many research and engineering fields, such as optical devices, geophysical inverse methods, applications to spacecraft dynamics. Modern ground vehicle dynamics have been developed based on the forward dynamics approach, which results in better understanding of kinematic response of vehicle subjected to applied forces. The control of vehicle performance can be achieved using inverse approach.

In inverse vehicle dynamics system, the output of actual vehicle is feedback to the inverse model (shown in Fig. 1.3) which is generally a controller whose input is predetermined. The vehicle's position is compared with the desired trajectory and the error signal is given to the controller to produce desired output.

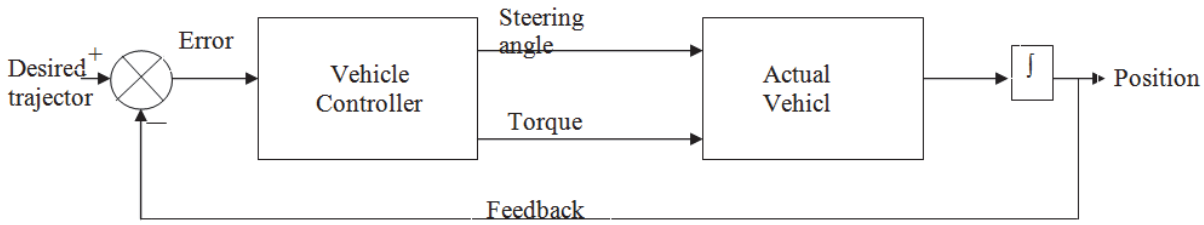

Fig. 1.3 Inverse vehicle dynamics control system

1.3 STEERING SYSTEM

The perfect steering is achieved when all the four wheels roll perfectly under all condition of running .While taking turns (Fig. 1.4), the condition of perfect rolling is satisfied if the axes of front wheels when produced meet the rear wheel axis at one point. This point is the instantaneous centre of the vehicle.

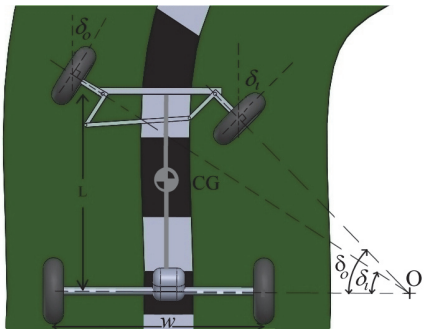

Fig. 1.4 Steering mechanism

It is seen that the inner wheel is required to travel through a greater angle (δ_i) than the outer wheel angle (δ_o). The equation for correct steering is given by

$$\cot(\delta_i) - \cot(\delta_o) = \frac{w}{L} \tag{1.1}$$

where w is centre to centre distance between rear wheels and L is centre to centre distance between front and rear wheels.

1.3.1 *Hydraulic Power Steering*

Two decades before when power steering technique was not popular, very large driving torque was required for driving the steering wheel. An external actuator is used to generate steering effort and this kind of system is called power steering. Hydraulic power steering (HPS) system was invented first. In hydraulic power steering, a pump provides assist force and hydraulic power steering system gives a straight line motion to rack and pinion mechanism to change the direction of wheel. The slight movement of the steering wheel actuates a valve so that fluid under pressure from reservoir enters the appropriate side of the cylinder and thereby, applying pressure on one side of the piston to operate the steering linkage which steers the wheel in the appropriate direction.

1.3.2 *Electrical Hydraulic Power Steering*

As technique progresses, a hybrid form of electrically controlled hybrid power steering system (HPS) was developed. In HPS, electrically controlled hydraulic valves are used. Electrically controlled Hydraulic power steering still has following problems:

- Hydraulic vanes leakage.
- Check and change of oil on regular time
- Hydraulic pump, hydraulic oil storage tank, vanes, valves increase weight and required large space.
- Response time is little more.

- Hydraulic pump draws power continuously from engine *i.e.*, fuel efficiency decreases.
- EPS system has fewer faults and is more durable as compared to HPS system.

1.3.3 *Electrical Power Steering*

Electrical power steering (EPS) system (Fig. 1.5) removes all above discussed problem. As there is no leakage problem in case of EPS, it is more eco-friendly. In electrical power steering, electric motor provides assistance to driver [**8**]. Electrical motor draws power when steering wheel moves and when wheel does not move EPS doesn't takes power. EPS system increases fuel efficiency. EPS system not only complete basic goal of power steering to reduce steering torque but also increases the driving satisfaction. EPS system draws power from battery and it does not depend on power drawn from the engine. As the commands and feedback signals of EPS system are electric in nature, its response is faster. A profound study is necessary for dynamic modelling of electrical power steering system.

As seen earlier, automobile industry has been changed a lot due to power steering. The leverage of large steering wheel is no longer required and as a result, the driver cabin could be designed with a more relaxed seating position. The hydraulic system not only reduces the steering effort, it also allows the quicker response. As invention continues, the size, cost and power requirements reduce dramatically. Now-a-days, power steering is a standard facility of almost each car.

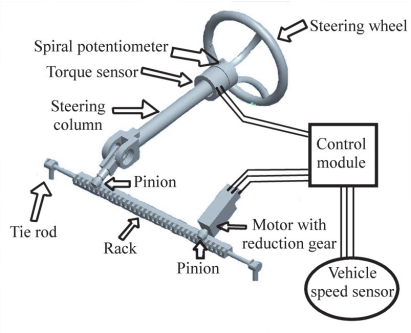

Fig. 1.5 Rack assisted electrical power steering

Even with all these refinements, power steering is still the same basic hydraulic system that was introduced 50 years ago. But for the first time in 1993, Honda introduced full time electric power steering in regular production car, Acura NSX. This is an exotic sports car, competing in the market with Ferrari and Porsche; later this, a small European market economy car, the Fiat Punto will have Delphi's electrically boosted E-STEER as standard equipment. Delphi is busily marketing their electric power steering system to the world's

automotive design engineers, and it is expected to show upon several domestic cars in just a few years. There are lots of advantages for using an electric motor to provide steering boost like better control, increased vehicle efficiency.

1.4 TYPES OF ELECTRICAL POWER STEERING

EPS are two types based on the electric motor position.

1.4.1 *Rack assisted electrical power steering*

In rack assisted electrical power steering (REPS) electrical motor gives assist effort to rack. More powerful motor is used in REPS (Fig. 1.6). The self-aligning moment intensity is more at the rack as compared to steering column due to rack and pinion gear ratio. REPS is useful for heavy vehicle.

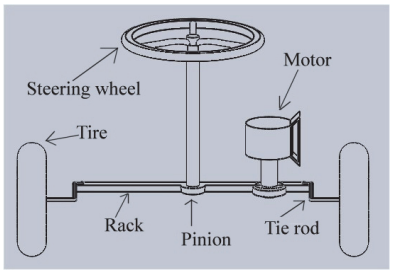

Fig. 1.6 REPS

1.4.2 *Column assisted electrical power steering*

The electric motor in mounted with steering column through gear pinion system. Electrical motor creates noise due to torque ripple. Torque ripple is the fluctuation in torque delivered by the motor. This reduces driver attention. Toque ripple is negligible in case of low power motor. Column assisted power steering is most suitable for light vehicle. CEPS Power requirement for CEPS is less as compared to REPS.

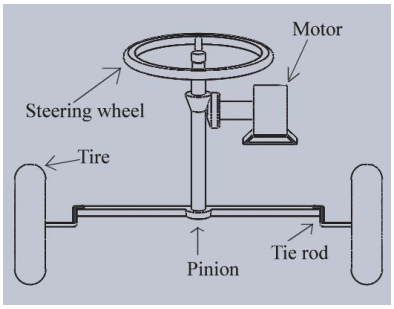

Fig. 1.7 CEPS

1.5 TYPES OF ACTUATOR IN ELECTRICAL POWER STEERING

The actuator used in electrical power steering is electric motor. For choosing the motor for EPS the motor torque ripple characteristics are very important. It affect the quality of output torque.

1.5.1 *DC motor*

It is a device that takes electrical energy and converts into mechanical energy to turn a shaft. In EPS system, DC motor is driven by battery. DC motor has starter of permanent magnet and a rotor that is rotated by attraction and repulsion with the starter. Rotor has an iron core fixed with the coil. Graphite bushes supply current to the coil with the help of commutation mechanism. Actual motor coil has not only inductance but it also has some resistance. The relationship between terminal voltage V_m, the impedance L, resistance R, voltage constant K, speed of revolution N, the current i and time t are given by

$$V_m = L.\left(\frac{di}{dt}\right) + R.i + K.N \tag{1.2}$$

In DC motor vibrations produces due to commutation mechanism. The motor is mounted near the driver in CEPS systems, and vibrations from around the dashboard are transmitted directly to the ears and to the hands of the driver through the steering column system. This means that motor noise is very likely to cause driver-disturbance. Motor should be powerful, have low moment of inertia and low loss of torque [**9**].

1.5.2 *Brushless DC Motor*

Brushless motor is very suitable to mount on in EPS system for saving energy. It does not take supply through commutation mechanism for vibration problem. The brushless DC (BLDC) motor has permanent magnet rotor. Permanent magnets are made-up with neodymium iron boron, ferrite, samarium cobalt and aluminium nickel cobalt. Cooper coils (starter) cover whole cylindrical surface of the rotor with small air-gap. The ON and OFF action occur sequentially between field coils by which the rotor rotates on its own longitudinal axis. The input voltage is of square wave form in BLDC motor. The different characteristics of both the motors are given in Table 1.1.

Table: 1.1 DC motor/brushless DC motor [**10**]

	DC MOTOR	Brushless DC MOTOR
Control	Armature	Square-wave
Inertia	High	Low
Friction	High	Low
Torque	Low	High

1.5.3 *Brushless synchronous motor*

The input voltage supply is sinusoidal wave form in Brushless synchronous (BLS) motor which has similar construction as BLDC motor. BLS motor has low rotary inertia, low weight as compared with similar capacity ordinary motor [**11**]. In BLS motor, torque ripple is generated by the harmonic content in electric voltage and electric current. Due to permanent magnet, no current torque is generated and this is undesirable.

1.6 BASIC BICYCLE MODEL OF A CAR

In a car model rear wheels are consider as a single rear wheel and front wheels consider as a single front wheel as shown in Fig 1.8. It has two DOF. Rolling pitch and their derivatives are set to zero. This model has following limitations:

- Model is limited to low speed motion.
- Large steering angle is not allowed to maintain cornering force linear.

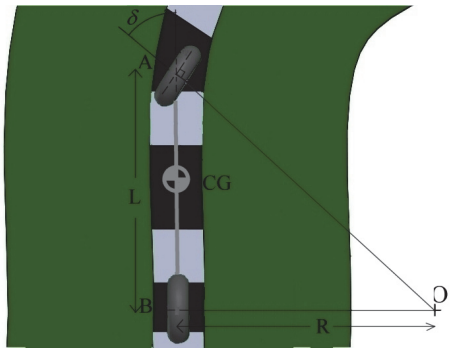

Fig 1.8 Bicycle vehicle model

In triangle OAB

$$\tan(\delta) = \frac{L}{R} \tag{1.3}$$

In the above equation, the turning radius is independent of vehicle velocity. This is called natural steering. In natural steering condition, centre of gravity (CG) always moves on a pure circular path with a constant steering angle. When bicycle vehicle model takes a turn the centrifugal force applies on CG. A side force causes a side slip angle [**12**].

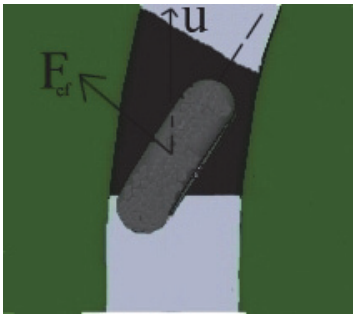

Fig 1.9 Cornering force

The function of side slip angle and cornering force is relates with tire stiffness as follows:

$$F_c = K \times \alpha \tag{1.4}$$

where K is tire stiffness and α is slip angle.

1.7 CONTROL ALGORITHM

The basic fundamental thing used for control of processes and objects in many fields of human activity is closed loop control. In the study of automatic control, the uncertain parameter like changes in inertial property (mass, moment of inertia) creates imperfections. When specifying a bicycle vehicle inverse model controller, the control algorithm is very authoritative characteristic that should be considered first. The control algorithm identifies the exact type of the output as a function of the input. The inputs to the algorithm are the trajectory paths. In bicycle vehicle model inertial parameters are uncertain.

- **Robust Overwhelming Controller**

A robust overwhelming controller for a bicycle vehicle which does not require the knowledge of the bicycle vehicle forward model parameters can be developed. The overwhelming control technique has been applied by researchers for robust trajectory control of robot. Robust trajectory control algorithms are useful here for developing an inverse vehicle dynamic model of bicycle vehicle model for following desired trajectory.

1.8 CONTRIBUTION OF THESIS

The contributions of the thesis are as follows:

- Bond graph model of bicycle vehicle model is developed.
- Bond-graph model of electrical power steering is developed.
- Driver control is replaced by electric motor in EPS.
- Inverse model of bicycle vehicle model is developed.
- Inverse model of EPS is developed.
- Inverse EPS and Bicycle vehicle model (controller) are attached with bicycle vehicle forward model.

1.9 ORGANIZATION OF THE THESIS

The thesis is organized in to 6 chapters, Short descriptions are as follows:

First chapter includes the introduction of inverse vehicle dynamics, construction detail of EPS, merits of EPS over HPS, bicycle vehicle model and controllers. Literature review

related to different algorithms of EPS, EPS modelling techniques, basic principles of Bond Graph and its applications in modelling of mechanical system and objective of thesis are included in the second chapter. Third chapter includes principle of work. Fourth chapter includes bond graph model of bicycle vehicle model, EPS and simulation results of bicycle vehicle model with EPS. Fifth chapter includes Bond Graph model of inverse bicycle vehicle model without inverse model of steering and with inverse model of steering. Conclusion and scope for future work are presented in the sixth chapter.

CHAPTER 2 LITIRATURE REVIEW

2.1 INTRODUCTION

This chapter includes the literature review on bond graph modelling of vehicle and electrical power steering system. The literature based on bond graph modelling of vehicle, vehicle handling dynamics and power steering is discussed. In electrical power steering various types of actuators and control strategies and sensor are used for making the electrical system more comfortable and safe.

2.2 BOND GRAPH MODELLING

Bond graph is a numerical tool to represent the systems structure. It is very flexible in modelling and formulates the equation of systems. Bond graph is formulation of classical system dynamics with many complicated structure and stimulates the imagination and abstract idea in integrated forms. Controller development for vehicles to improve the fuel efficiency, performance, handling and safety. Digital spark ignition, anti-lock braking system, automatic gear changer are the example of latest vehicle technologies. These all are based on some control algorithms. The controller development requires sensors, actuators, signal processing. A vehicle model with all these parts is required to judge the control law developed by researchers. Bond graph is a pictorial method to model vehicle model with sensors, actuators, signal processing. Bond graph is suitable for modelling an electronic control and electrical actuator attached with mechanical vehicle model. In bond graph system models are represented by symbols, lines and power flow information [**13, 14**].

To develop the control algorithms for road vehicle, rail vehicle, high speed complex large machines, machine tool or industrial robots, modelling and simulation is an inexpensive method. The large mechanical systems built up by finite number of rigid bodies interconnected by arbitrary joint. The study rotational or translational motion damping, compliance, inertial properties of subsystem are required. In classical mechanics many method are exist by which system differential equation can be derived for a system. Classical mechanics methods are labour-intensive and consequently error prone [**15**]. Bond graph is a unified and graphical method to represent dynamic systems. Bond graph is based on the fact that physical system can express in term of four generalized variables effort, flow, displacement and momentum [**16**]

Vehicle design and development is a costly and time consuming process. Vehicle development process requires a comprehensive analysis of system to determine the dynamic

characteristics. In case of hybrid power trains vehicles development process becomes more time consuming and clumsy due to complexity and large number of subcomponent. In bond graph, system models are developed by consideration of energy flow and easy for modelling the hybrid systems. Bond graph model denotes subsystems, system component and element connected by power bond. The nodes of the power bonds called power port at which energy can enter or leave. Bond graph model provides a lot of information about mathematical model and has ability to transform in mathematical models like as transfer function, Lagrange equations, descriptor equation if needed. Bond graph is easy method for a modular modelling and hierarchical modelling is possible by coupling the component and subsystems through their connecting ports. Bond graph is allows both causal and behavioural process analysis.

2.3 BOND GRAPH MODELLING OF VEHICLE

Bond graph modelling is widely used in vehicle dynamics. Bond graph is most suitable for control algorithms development, optimization and analysis of vehicle. A unicycle model is developed by bond graph modelling [**17**].

This unicycle model is extended in four wheel model with some assumption. Model has independent electric brake actuator, a steering actuator and suspension at each corner of vehicle. Differential mechanics is used between steering column and steering assist motor. Steering moves according to driver command without reaction force on driver‘s hands [**18**].

The four wheel vehicle model controlled with different control algorithms are modelled by bond graph modelling technique. Vehicle model included with roll, yaw degree of freedom, tire reactions, and yaw slip angle. This model can be a base model for developing controller for vehicle handling and safety analysis [**19**].

A bond graph model of full vehicle with electrical actuator is described. The vertical, longitudinal and lateral vehicle dynamics are included with suspension system. Pacejka model is also considered with model. Each wheel is tracked with independent actuator [**20**]. Vehicle model with suspension system, engine, transmission and accelerator included to analyse the vehicle traction is discussed, model has three degree of freedom with non-linearity. Pacejka model for the tire pneumatic characteristics is also considered [**21**].

An integrated hybrid vehicle system is developed with model reduction algorithm. This reduced model is helpful to vehicle design optimization [**22**].

The vehicle safety system can be more effective if the variable of vehicle are well known. A model is developed which is divided in two blocks for observing tire forces and slip angle. Block one indicates vehicle body dynamics and second block indicates dynamics of tire road interface. Block one computes tire forces and yaw rate and second block computes side slip

and tire cornering stiffness. The linear adaptive force model is also described to correct errors results from road friction changes [**23**].

The intelligent transportation system, antilock braking technology which are useful to avoid the road accident. To increase safety improvement in steering performance is also required. A multi body model for tire road interaction is developed by bond graph approach. This model is used to develop a robust fault detection and isolation algorithm. This algorithm improves vehicle safety [**24**].

Independent axle torque biasing technique is discussed. ITB directly controls the yaw rate, improves vehicle steer-ability and stability [**25**].

2.4 BOND GRAPH MODELLING OF ELECTRICAL POWER STEERING

Component of EPS system are steering wheel, steering. Torque sensor is mounted with steering column; another end of steering column is connected with gearing mechanism. Torque sensor gives a signal to control module. Reduced order modelling is used. Close loop transfer function is drawn to understand the basic requirement of EPS. Assist algorithm, return algorithm and damping algorithm are proposed. Assist algorithm is designed with consideration frictional and inertial compensation. Steering wheel must be return after achieving desired yaw moment of vehicle and damping algorithm prevent the overshoot [**26**].

Control module receives signals from five sensors engine speed sensor, vehicle road speed signal, torque sensor signal, position sensor, and rack moment sensor. Depending on the steering force, road speed, engine speed, steering angle, steering speed and maps stored in the control unit, the control unit calculates the necessary assisting force and actuates the electric motor.

Performance parameters of EPS system are response time, stability. Vehicle response with change in steering wheel torque plays very important role in study of EPS system output. Vehicle response also depends on tyre pressure, road condition and weight distribution on vehicle [**27**].

Torque sensor is essential component of EPS. Conventional torque sensor are potentiometric, optical used in EPS. Torsion bar shown angular displacement according to applied torque. Torsion bar can use as a torque sensor in EPS. Mechanical compliance of torsion bar helps to maintain stability of EPS [**28**].

Lose in vehicle control of wet or icy road can be prevented by using yaw rate feedback. Without yaw rate feedback sensor vehicle stability depends on the ability of driver

to track lateral velocity changes. EPS handling characteristics improves with yaw rate feedback sensor [**29**].

A diagnostic algorithm developed to help design appropriate operation for vehicles during steering related failures. The driver model developed using experimental data. Driver applied required torque with considering self-aligning forces acting on front wheel. Path deviation increases as a function of vehicle speed. Unwanted steering is a mode of failure when EPS gives output without a steering input from driver [**30**].

Exhibit robustness and stability problem for certain road conditions. Neural network with PID controller has ability to stay stable in any operational conditions, EPS response and sensitivity improves with neural network. Simulation is done on MATLAB [**31**].

A road surface information sensitive EPS system design discussed. This EPS system got information of road surface by frequency separation. Mechanical components such as reduction gear, pinion, torque sensor also discussed and feasibility test of design was confirmed by experiment [**32**].

A linear electrical power steering system with PD controller is proposed. Vehicle handling and stability was improved with keeping constant differential coefficient of PD controller constant and increasing proportional coefficient of PD controller [**33**].

An intelligent steering system is discussed. A controller have information of all wheels angular position (yaw) by absolute encoded. All wheel are steered by simultaneously or sequentially steered. This unique steering system allows a totally different parting system in urban areas. This innovative design may useful in mobile robots. Intelligent steering system is more efficient than conventional steering system. Torque difference between four wheels can steer the vehicle. Steering such system it is extremely important to balance the torque at all wheels in a manner that slip angle should be completely zero [**34**].

Power wheeled steering method by using two driver wheels is developed. An efficient controller is proposed for PWS method. Controller includes a feel forward compensator that have inverse dynamics of vehicle and controls the position of both sides of wheels and also controls the velocities of wheels [**35**].

An analysis and design of a dual pinion type sensor less EPS control system is discussed. An optimal controller based on lagrangian dynamics is proposed. Linear quadratic regulator (LQR) and kalman filter method is used to get optimal controller for EPS system. The torque sensor at steering column increases stiffness of steering column and increases steering feel [**36**]

A model for EPS system is proposed for power saving. EPS system gives power to provide the steering torque to wheels. This torque should be more than self alignment torque of wheels. In this model the self aligning torque is used to recover the energy needed to steer the wheel. Discussed model can easily embedded with existing EPS system and vave ability to save 20% power [**37**].

A torque sensor less EPS system is discussed. A step by step high order sliding mode observer (HOSMO) measures driver torque by rack force feed-back. It is more effective because torque sensor on steering column increases steering column stiffness [**38**].

A steer by wire (SBW) system is discussed. SBW system is more safe and comfortable as compare to traditional power steering. The model of mechanical parts and control unit of SBW is developed by bond graph modelling. Controller receiver column steering torque sensor signal and steering wheel angular position sensor. System has three main parts, one is steering wheel with torque sensor and angular position sensor, second is electric motor and third one is controller with vehicle speed sensor, yaw rate sensor and accelerator sensor. Result shows Front wheel angle is a function of steering wheel angle and vehicle speed [**39**].

In bond graph modelling system is divided in compliance, inductance, resistance, power sources, transformer, and gyrator. A bond graph model of electrical power steering is developed. It was observed that a signal filter is necessary in between steering column torque sensor and controller. Result validates the effectiveness of EPS Simulink model [**40**].

By the study of literature of EPS a bond graph model can develop as follows

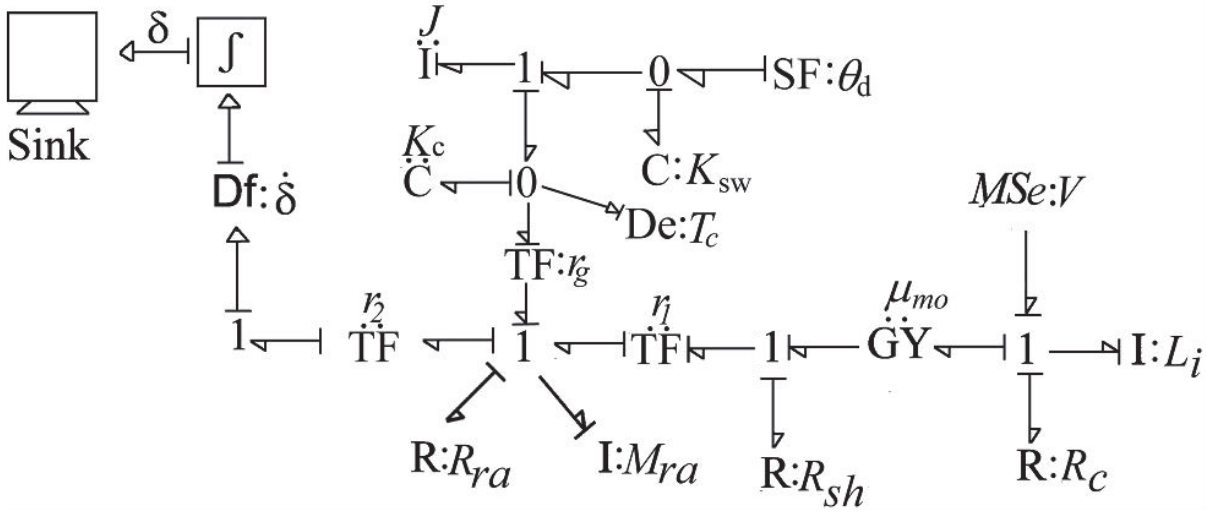

Fig. 2.1 Bond graph model of EPS

The EPS bond graph model shown in Fig. 2.1, θ_{d} driver input steering wheel and δ is the output of the system. K_{sw} is the steering wheel stiffness, K_{c} is steering column stiffness, J is steering wheel moment of inertia. Electrical motor provides assist torque T_{a} . Motor input voltage is V . Motor coil resistance and inductance are R_c and L_i. μ_{mo} is motor constant which converts electric current in to mechanical torque T_{m} and R_{sh} motor shaft damping coefficient. Rack mass and damping are M_{ra} and R_{ra} respectively. r_g , r_1 , r_2 are reduction gear ratio, ball screw reduction ration and steering linkage ration. An effort detector is attached at column to measure the steering column torque. Torque measured by torque sensor,

$$T_{\mathrm{c}} = T_{\mathrm{d}} - J.\ddot{\theta} \tag{2.1}$$

Motor torque,

$$T_{\mathrm{m}} = i.\mu_{\mathrm{mo}} \tag{2.2}$$

Assist torque,

$$T_{\mathrm{a}} = T_{\mathrm{m}} - \theta_{\mathrm{sh}}.R_{\mathrm{sh}} \tag{2.3}$$

2.5 LITERATURE GAP

After doing brief study of literature on EPS, vehicle handling and bond graph modelling, it is known that many researchers work on EPS in which driver exists in control loop. In bond graph model is the output of EPS system and driver a command and assist motor provides assist torque. Steering angle for any given path can easily computed. Many algorithm related to path tracking and obstacle avoidance are available in literature. The inverse model of EPS system can be useful to compute the steering wheel toque. According to literature steering angle not only a function of steering wheel torque. Steering angle also depends on vehicle speed. Since an inverse vehicle model is necessary to develop a controller for autonomous vehicle modelling. As per my knowledge, there are very few literature is available for inverse vehicle controller. Various path coordinate generation techniques are available in literature. In EPS system, the driver can be replaced by an inverse bicycle model with the help of path coordinate.

2.6 OBJECTIVE OF PRESENT WORK

According to the literature review, it is found that bond graph modelling is useful for modelling the vehicle handling algorithm and simulation of vehicle model. Bond graph is

best suitable method to model the mechatronics systems. Objective of this thesis is to develop an inverse vehicle dynamic model of bicycle with power steering. Bicycle vehicle model for which path coordinate will be the input and steering angle, vehicle longitudinal velocity will be the output although motion control of vehicle is very difficult task because many uncertainties such as load variation, friction between tire and road surface and external disturbances. These exhibit robustness problem can be solved by robust overwhelming controller. Robust overwhelming controller technique is one of the most effective to handle such uncertainty. Manny researchers used this technique in robot manipulators. The inverse vehicle dynamic model of a bicycle vehicle with power steering will attached as a controller with forward bicycle vehicle model with robust overwhelming controller. By the use of inverse bicycle model safety, traffic management improves and inside space of vehicle increases.

CHAPTER 3 PRINCIPLE OF WORK

3.1 INTRODUCTION

In this chapter modelling and simulation by bond graph modelling is discussed. Modelling and Simulation is an important task to analyse the system that is not physical built. Simulation of system and surrounding gives the information of system dynamic, ensures safety of the system and avoids cost of redesign. Bond graph modelling maps the effort and flow. Power is time derivative of energy since flow energy in a system can easily calculated by study of power in a system. Power is convenient entity to model the system built with multiple domain. The multidisciplinary system can easily analysed by bond graph methodology. This modelling technique is based on the fundaments of power flow between nodal elements.

$$power = flow \times effort \tag{3.1}$$

The bond graph modelling procedure is graphical nature by which it is easy to grasp. Subsystem can defines in the form of words in bond graph. This type of bond graphs are known as word bond graph. Word bond graph is a graphical way to visualise the power flow between components of a large system [**41**].

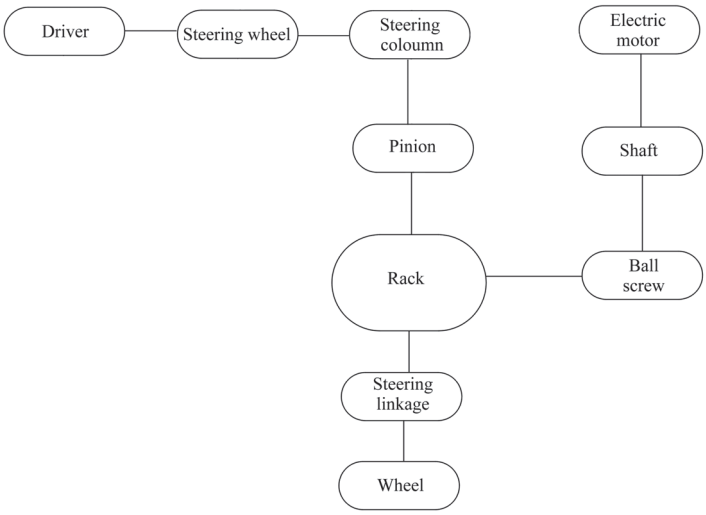

Fig 3.1 Word bond graph of REPS

3.2 BOND GRAPH

Power flow between two junctions is represented by power bond in bond graph modelling. Fig.3.1 shows a half arrow power bond symbolizing the power flow from junction 1 to 0.

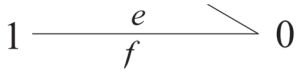

Fig. 3.2 Power bond

Power bond has two variable one is flow variable other is effort variable. Fig.3.2 represents the effort and flow variables with e symbol on the harpoon side of the bond, representing the effort, and f symbol on the opposite side, representing the flow. Electrical, hydraulic, mechanical, thermal or chemical systems are deals with similar manner in bond graph. Table 3.1 shows the effort and flow variable in different-2 energy domain.

Table: 3.1 Effort and flow variable in Different system

SYSTEM		**EFFORT**	**FLOW**
MECHANICAL	Translation	Force	Velocity
	Rotation	Torque	Angular velocity
HYDAULIC/PNEUMATIC		Pressure head, Pressure	Weight flow rate, Volume flow rate
THERMAL		Temperature	Heat flow rate
ELECTRICAL		Voltage	Current
CHEMICAL		Enthalpy	Mass/mole flow rate

The block diagrams, differential equation and signal flow graphs can also draw for any kind of physical system by his bond graph model.

3.2.1 Junction

Power bonds are connected together at junctions. There are two types of junctions in bond graph modelling. Each of the junction types are set up such that the amount of power coming into the junction equals the amount of power leaving the junction. No creation of power, or power storage, is allowed in a bond graph junction. The first type of bond graph junction is referred to as a zero-junction. Each of the power bonds connected to a zero junction have equal effort terms. The flow terms of the power-bonds connected to the zero junction sum to zero, *i.e.*, $f_{01} - f_{02} - f_{03} + f_{04} - f_{05} = 0$ and $e_{01} = e_{02} = e_{03} = e_{04} = e_{05}$, shown in Fig. 3.3.

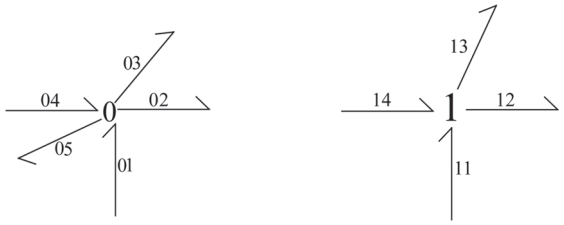

Fig. 3.3 Junction

The second type of bond graph junction is a one-junction. The power bonds connected to a one junction have equal flow terms. The effort terms of the power bonds connected to the one junction sum to zero, *i.e.*, $f_{11} = f_{12} = f_{13} = f_{14}$ and $e_{11} - e_{12} - e_{13} + e_{14} = 0$, shown in Fig. 3.3. Each junction may have an unlimited number of power bond connections. The power bonds, on each of the junctions in Fig. 3.3, are arbitrarily numbered to keep record of the conjugate variables associated with them. Power bonds in a bond graph may be numbered sequentially. However, one need not follow any fixed rule. It is clear from Fig. 3.3 that each type of junction conserves power in such a manner that power into the junction is equal to the power out from the junction. By holding one of the conjugate variables equal on all bonds connected to the junction, the other conjugate variable must then sum to zero, *i.e.*, incoming minus outgoing equals zero.

Bond graphs use two energy source elements flow source and effort source. These elements have one port. Three other one port elements are R, C and I which represent resistance, capacitance and inductance of the system respectively.

- **R Elements:**

The 1-port resistor is an element in which the effort and flow variables at the single port are related by a function (Eq. (3.2)). Generally resistors dissipate energy. This must be true for simple electrical resistors, mechanical dampers or dashpots, porous plugs in fluid lines, and other analogous passive elements. The bond graph symbol for the resistive element is shown in fig. 3.4.

$$f = \frac{e}{R} \tag{3.2}$$

- **I Elements:**

A second energy storing 1-port arises if the momentum, P, is related by a static constitutive law to the flow, f. Such an element is called an inertial element in bond graph terminology. The inertial element is used to model inductance effects in electrical systems and mass or inertia effects in mechanical or fluid systems. The bond graph symbol for an inertial element is shown in the Fig. 3.4.

$$f = \frac{1}{I}\int_{-\infty}^{t} e dt \tag{3.3}$$

- **C Elements:**

Consider a 1-port element in which a static constitutive relation exists between an effort and a displacement. Such a device stores and gives up energy without loss. In bond graph terminology, an element that relates effort to the generalized displacement (or time integral of

flow) is called a one port capacitor. In the physical terms, a capacitor is an idealization of devices like springs, torsion bars, electrical capacitors, gravity tanks, and accumulators. The bond graph symbol for a capacitor element is shown in the Fig.3.4. The expression for this bond graph symbol K is defined as,

$$e = K\int_{-\infty}^{t} f dt \tag{3.4}$$

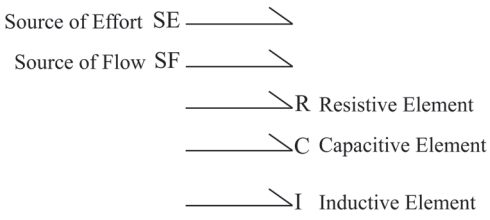

Fig. 3.4 Single port elements

Two types of two port element exist in bond graph modelling one is transformer (TF) and other is gyrator (GY). Elements TF and GY neither stores power nor dissipates. Mostly these elements are used to model the boundary of two different-2 engineering domains. Elements R, C, I, TF and GY do not contain power source. These are also called as passive element and SE, SF are call as active elements.

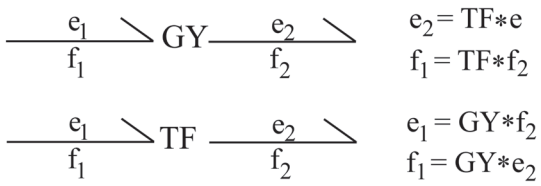

Fig. 3.5 Two port elements

- **TF Element:**

An ideal transformer is represented by TF. The transformation can within the same domain (gear box) or between different domains (electric motor), see Fig. 3.6.

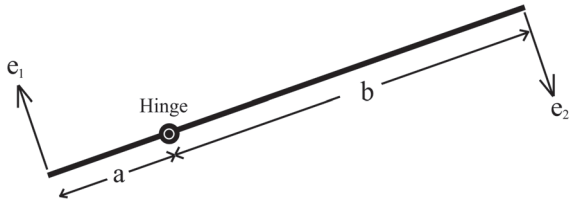

Fig. 3.6 Lever

The equations are:

$$e_1 = \left(\frac{a}{b}\right) e_2 \tag{3.5}$$

$$f_2 = \left(\frac{a}{b}\right) f_1 \tag{3.6}$$

Efforts are converted to efforts and flows to flows. The parameter a/b is the transformer ratio. Due to the power continuity, only one dimensionless parameter a/b is needed to describe both the effort transduction and the flow transduction.

- **GY Element:**

An ideal gyrator is represented by GY, and is also power continuous (*i.e.*, no power is stored or is dissipated. Examples are an electromotor, a pump and a turbine. Real–life realisations of gyrators are mostly transducers representing a domain–transformation (Fig. 3.7). The equations are:

$$e_1 = \mu . f_2 \tag{3.5}$$

$$e_2 = \mu . f_1 \tag{3.6}$$

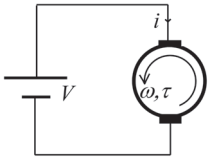

Fig. 3.7 Electric motor

Equation for the system shown in Fig. 3.7

$$V = \mu . \omega \tag{3.8}$$

$$\tau = \mu . i \tag{3.9}$$

V is the supply voltage , i is current in circuit, ω is angular velocity of motor and τ is output torque on motor shaft. The value of gyrator is μ which convert electrical flow in to mechanical effort. This is also known as motor constant.

Figure 3.3 shows a mass spring damper system associated with a cam. Cam shaft is moving with angular velocity ω, mass of block is M, spring stiffness is K and damping coefficient is R.

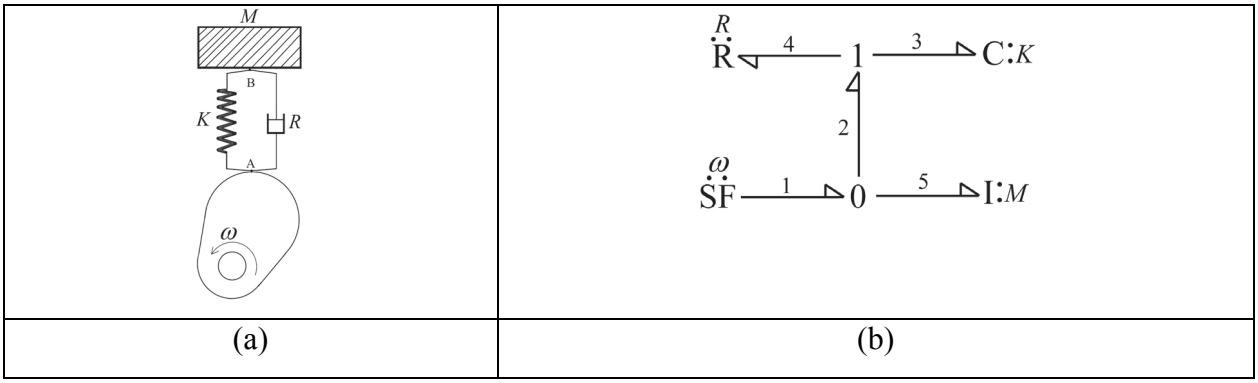

(a) (b)

Fig. 3.8 (a) Cam with ICR (b) Power flow diagram of cam with ICR

In Fig. 3.6 the cam is a source of flow for system. Spring and damper have same velocity at point A. Flow is distributed in between spring, damper and mass at point B. In Fig. 3.7 spring and damper are connected with one junction (for point A) and inertial element is connected with zero junction [**16**].

3.2.2 Causality

Once effort and flow variables and power flow direction have been assigned, equations may be written from the bond graph. However, more information may be added to the bond by assigning input and output variables at a port, that is, by assigning causality. The effort and flow variables on a bond will be assumed uniformly to be oppositely directed. Therefore, causality may be assigned by placing a single line across one end of the bond as shown. Causality is used to show the direction of effort and flow information for each bond in power flow diagram [**14**]. In Fig 3.7(b) the power flow diagram did not assign causality.

Table: 3.2 Causality for basic port elements

ELEMENT	CAUSAL FORM	CAUSAL RELATION
Source of effort	SE ⟶	$effort = e(t)$
Source of flow	SF ⟶	$flow = f(t)$
Resistance	⟶ R	$effort = flow/R$
	⟶ R	$flow = effort * R$
Capacitance	⟶ C	$e = K\int_{-\infty}^{t} fdt$
Inductance	⟶ I	$f = \frac{1}{I}\int_{-\infty}^{t} edt$

Transformer		$e_1 = TF * e_2$ $f_2 = TF * f_1$
		$e_2 = \frac{e_1}{TF}$ $f_1 = \frac{f_2}{TF}$
Gyrator		$f_1 = \frac{e_2}{GY}$ $f_2 = \frac{e_1}{GY}$
		$e_1 = f_2 * GY$ $e_2 = f_1 * GY$
Zero junction	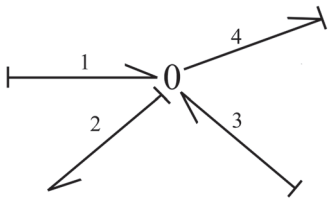	$f_1 - f_2 + f_3 - f_4 = 0$ $e_1 = e_2 = e_3 = e_4$
One junction	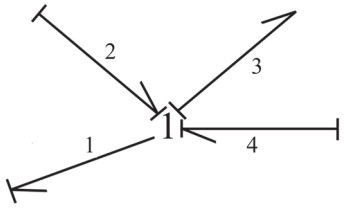	$f_1 = f_2 = f_3 = f_4$ $-e_1 + e_2 - e_3 + e_4 = 0$

At one junction only one power bond brings the flow information. Similarly at zero junction only one bond has effort causality. These uniquely causalled power bond is called strong bond. More than one strong bond is not allow at a junction in bond graph modelling.

3.2.3 Activation

In bond graph the activated bond are expressed by double arrow head tied to the middle of the power bond. These activated bond carry only one power conjugated variable either flow or effort [**30**]. There are two kind of activated bond.

3.2.4 Sensor and Actuator

Sensor are needed to scenes the system response. Sensors takes very small amount without affecting the system. If the dynamic characteristics of a sensor can neglected, then sensor can be modelled by an energy sink that provides a zero flow. In bond graph modelling ideal

sensor are very effectivity used. An integrally causalled C element detect the flow and integrally causalled I element detect effort. Flow detector is shown by Df and effort detector is shown by De. These detectors are connected on junction with weak bond. Flow detector is connected at 1 junction and effort detector is connected at zero junction.

Source element provides power for the system in terms of flow or effort that is constant or time dependent. Somewhere source elements may be controlled by a signal comes from sensor. This type of source are called modulated source and its output depends on modulating signal. Two ports element can also be modulated. The value of TF and GY modulates with signal. If signal is more value of TF will be more if modulating signal is low the value of TF will be low.

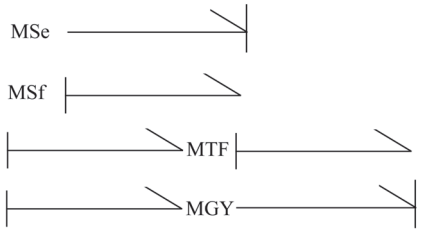	Modulated source of effort Modulated source of flow Modulated transformer Modulated gyrator

Fig. 3.9 Modulated element

3.2.5 Differential Causality

Junction elements do not have more than one strong bond. Causal stroke in R element can place in head side or tail side on power bond, this flexibility of R element avoid that situation. Model showing the reverse causality orientation can be avoided without using extension or reduction of model. Integral causality means the past data of cause ($e = K\int_{-\infty}^{t} fdt$ limit is past to present) while differential causality needs differentiation of the cause at present that cannot be found properly. Differential casualty makes the system dynamics dependent on future.

3.2.6 Example of assignment of causality

Bond graph of system shown in Fig. 3.7 with causality is drawn (Fig. 3.9) as

- Step 1: Define the fixed causality for source element.
- Step2: Assign the causality at zero junction. Define the causality for I element.
- Step 3: At zero junction bond 5 is known. Zero junction must have one strong bond so define the causality of bond 2.
- Step 4: Assign the causality at one junction. Define the causality for C element.
- Step 5: At one junction bond 2 is strong bond since bond 4 should be weak bond.

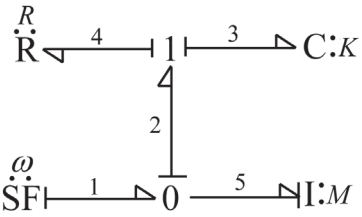

Fig. 3.10 Causality of Cam with ICR

The system governing equation can also generated by step by step procedure through the bond graph. Bond graph shown in Fig. 3.9 differential equation can be generated as follows:

Source element gives flow ω. Zero junction is flow summing junction and effort at this junction will be same. Flow in bond 5 will be P_5/M where P_5 is momentum of I element.

$$f_2 = f_1 - f_5$$

$$\Rightarrow f_2 = \omega - \frac{P_5}{M} \tag{3.8}$$

$$e_1 = e_2 = e_5 = \frac{dP_5}{dt} \tag{3.9}$$

One junction is effort summing junction and flow will be same in all associated bonds ($f_2 = f_3 = f_4$). R element returns effort at bond 4 is $R \times f_2$ and C element returns effort $K \times Q_3$, where Q_3 is displacement in spring.

$$e_2 = e_3 + e_4$$

$$\Rightarrow \frac{dP_5}{dt} = e_3 + \left(\omega - \frac{P_5}{M}\right) \times R$$

$$\Rightarrow e_3 = \frac{dP_5}{dt} - \left(\omega - \frac{P_5}{M}\right) \times R$$

$$\Rightarrow K \times Q_3 = \frac{dP_5}{dt} - \left(\omega - \frac{P_5}{M}\right) \times R$$

$$\Rightarrow \frac{dP_5}{dt} = K \times Q_3 + \left(\omega - \frac{P_5}{M}\right) \times R \tag{3.10}$$

3.3 EXAMPLE OF MASS SPRING DAMPER SYSTEM

The mass spring damper with a cam shown in Fig. 3.8. The cam gives power to the system and mass M gets effort through the system and makes oscillatory motion, since input in the

system is effort and output of the system is oscillatory flow of mass M . Spring stiffness is K and damping coefficient is R. Gravitational force on mass M is $M \times g$ in vertically downward. Mass, spring and damper are represented by I element, C element and R element. The bond graph model of this system (3.8) is drawn as following steps,

- Cam gives power to system as a source of flow.
- At point A the spring and damper has same flow since C element and R element will connect with one junction.
- Flow is distribute at point B since spring damper subsystem and source of flow and I element will connect with zero junction.
- Gravitational force applies on mass M since a source of effort will connect with I element.

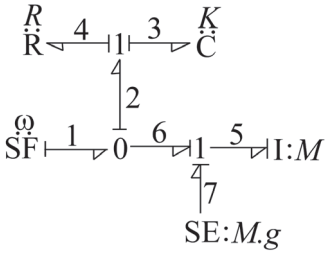

Fig. 3.11 Cam ICR bond graph with gravitational force

In Fig. 3.10 bond graph model it is seen mass M get effort from rest of the system and returns flow. SF element gives flow to the system, this flow is distributed at zero junction. Spring damper subsystem returns effort. This effort and gravitational effort added at one junction and goes to I element, I element returns flow to the system.

3.4 INVERSE OF MASS SPRING DAMPER SYSTEM

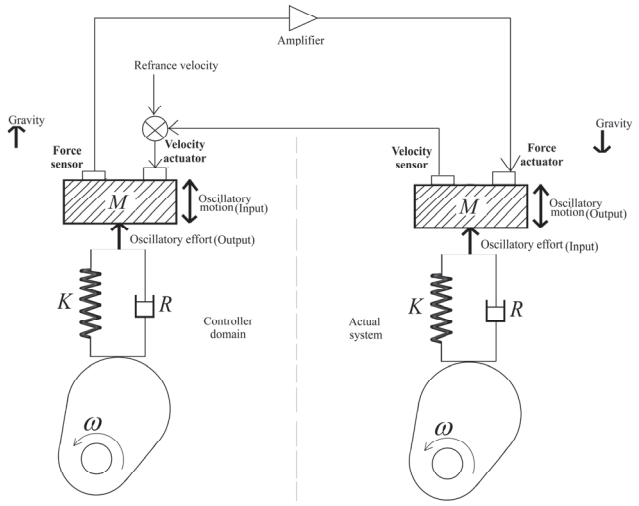

Fig 3.12 Cam with ICR, forward and inverse model

The controller model flow is input and effort is output. Effort amplifies and goes to actual model. Flow returns to controller as a feed-back. The bond graph of actual system and virtual system (controller) is shown in Fig. 3.11.

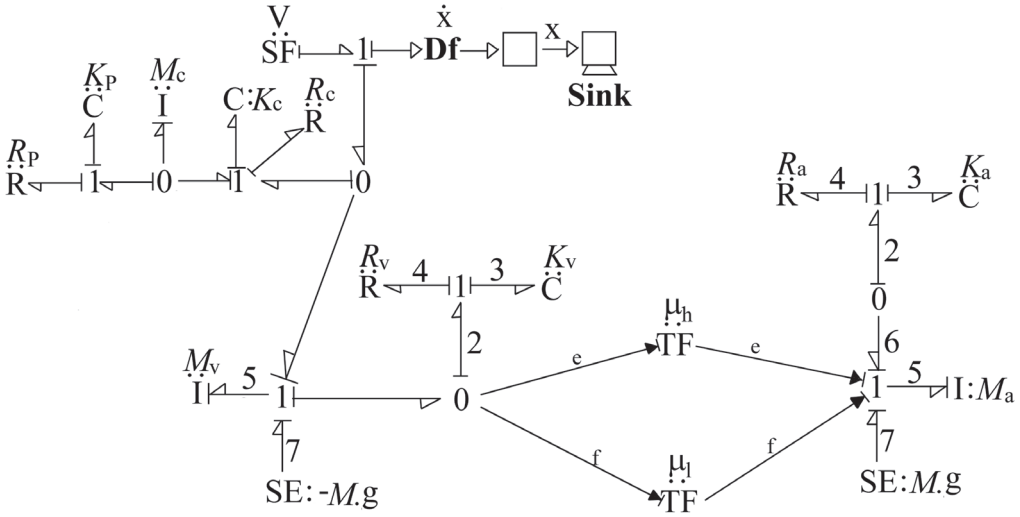

Fig. 3.13 Cam ICR inverse and forward model with overwhelming controller

The M_V, K_V, R_V are the virtual mass, virtual stiffness and virtual damping coefficient respectively. Ma, Ka and Ra are the mass, stiffness and damping coefficient of actual system. R_P and K_P are the pad damping and stiffness to avoid differential causality. M_C, K_C and R_C are the ghost controller virtual mass, damping and stiffness.

Table: 3.3 Spring mass damper simulation parameters

PAPAMETER	Value	PAPAMETER	Value	PAPAMETER	Value
ACTUAL MODEL PARAMETER		VIRTUAL SYSTEM PARAMETER		GHOST CONTROLLER PARAMETER	
Mass *M*a	5	Mass M_V	20	Mass M_C	1
Stiffness *K*a	1e10 N/m	Stiffness K_V	1e8 N/m	Stiffness K_C	1e8 N/m
Damping coefficient *R*a	0.5 Ns/m	Damping coefficient R_V	0.4 Ns/m	Damping coefficient R_C	1e4 Ns/m
Gravitational acceleration *g*	9.8 Kg/N	Gravitational acceleration *g*	9.8 Kg/N	Pad stiffness K_P	1e11 N/m
Gain μ_h	100	Gain μ_l	1	Pad damping coefficient R_P	10 Ns/m

Result shown at $M_a = 5$ and at $M_a = 10$ response of actual system is same since independent to actual model parameter.

$$\text{Input velocity } V = \begin{cases} 40 & t < t_1 \\ 80 & t \geq t_1 \end{cases} \tag{3.11}$$

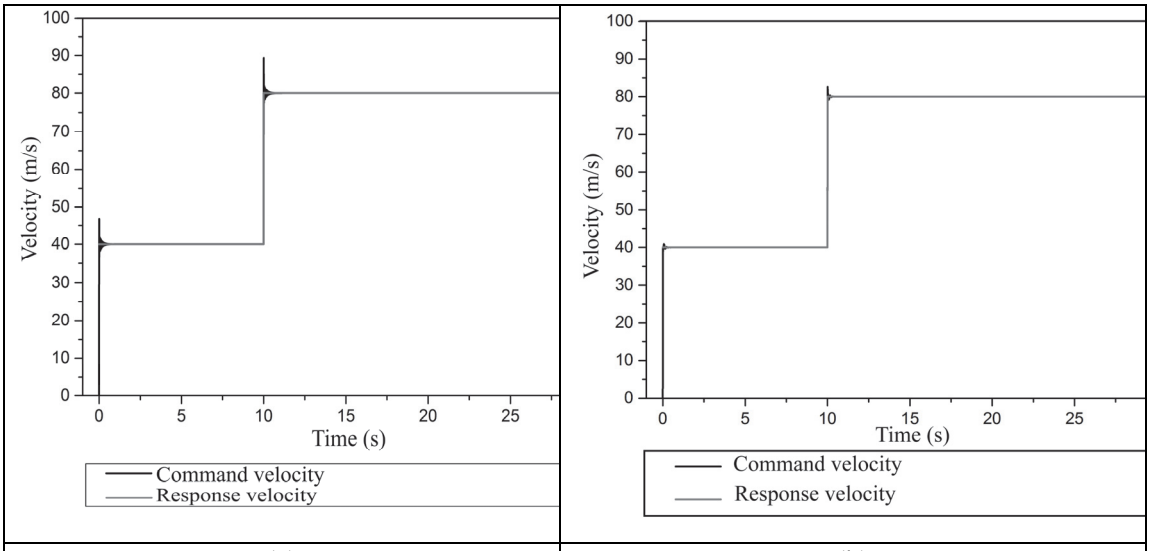

Fig. 3.14 Cam ICR command and response

Figure 3.12 shows velocity vs time graph of controller and actual system at plant mass 5 kg and Fig 3.13 shows velocity vs time graph of controller and actual system at plant mass 10 kg. The system parameter is change but actual response always follows the command of controller. This overwheelming controller can implement on vehicles. In this simulation gain μ_h is 100. If μ_h is higher response comes closer to command value.

CHAPTER: 4 DEVELOPMENT OF FORWARD MODEL

4.1 INTRODUCTION

This chapter introduces the bicycle vehicle model with electrical power steering and manual steering. Bond graph model of bicycle vehicle model, manual steering model and power steering model are developed. In bond graph model of EPS and bicycle model a capsule (sub model) of electric motor is used. In bicycle vehicle model the roll is not considered. There is no suspension system in bicycle vehicle model and bicycle vehicle model is moving on plane surface since pitching motion is not considered, only steering effect on bicycle vehicle model is studying in this chapter. Driver model in steering bond graph model is considered as an idea power source. Electric motor is considered an ideal motor which has no torque ripple and no cogging torque. A comparative study of manual steering and EPS is done. Result shows EPS gives better response as compare to manual steering.

4.2 PLANAR VEHICLE MODEL

A bicycle model of vehicle used for the vehicle handling study with manual steering system and electrical power steering system. There is no roll and sway motions, only yaw motion is considered. This bicycle vehicle model is front wheel steering model. The steering system attached with front wheel of bicycle vehicle model, steering angle is δ shown in Fig. 3.1. The angular displacement due to yaw motion of vehicle is shown by θ_z. The bond graph model of this bicycle vehicle model is shown in Fig. 3.2.

The bond graph model of bicycle model of vehicle is a standard example, which is available in introductory chapter of any bond graph modelling book. This is assumed steering is applied on constant velocity and there is no externally acceleration or retardation at the time of steering. When steering is applied the longitudinal velocity of vehicle goes down but power applied on rear wheel do not change. There is no over or under steering. Steering wheel rotates some angle and vehicle takes a turn of constant radius. The distance between front and rear wheel from the centre of gravity of vehicle is l_1 and l_2 respectively. Rear wheel rotates by external source (electric motor capsule) and makes a push to centre of gravity of vehicle. The Pacejka model is used to model the road tire interaction, which gives the value of rolling resistance of rear and front wheel. The Pacejka model considers in terms of tire cornering force and slip angle.

$$Slip\ angle = a\tan\left(\frac{v}{u}\right) \tag{4.1}$$

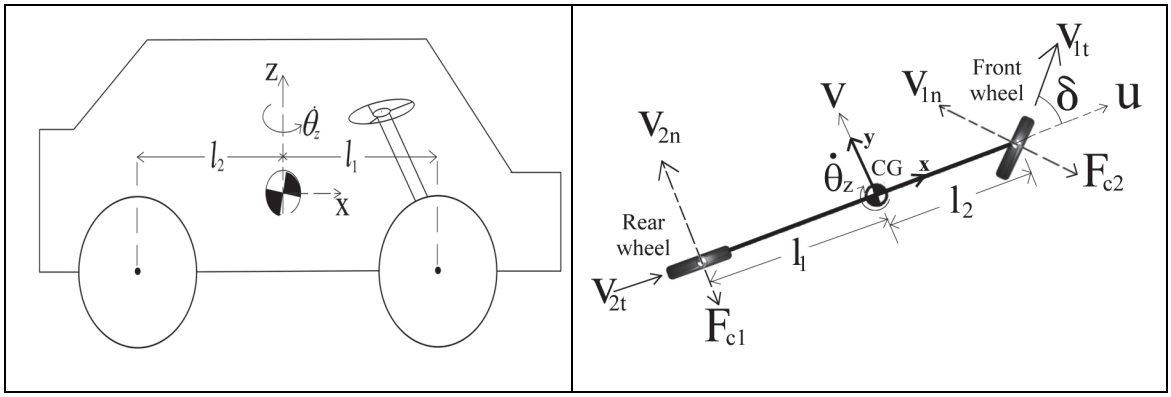

Fig. 4.1 Bicycle model of vehicle

4.3 KINEMATIC RELATION

Bicycle vehicle model shown in Fig 4.1, CG is the centre of gravity, x-y is the local coordinate system of vehicle. Vehicle is moving with u velocity, steering angle in front wheel is δ. The bicycle vehicle model takes a turn with angular velocity ω_Z $(d\theta_z/dt)$ about z axis. F_{c1} and F_{c2} are the cornering forces in front and rear wheel respectively. Therefor normal and tangential velocity of front wheel,

$$\left.\begin{aligned} v_{1n} &= \left(v + \dot{\theta}_z l_1\right)\cos\delta - u\sin\delta \\ v_{1t} &= \left(v + \dot{\theta}_z l_1\right)\sin\delta + u\cos\delta \end{aligned}\right\} \tag{4.2}$$

And normal and tangential velocity of rear wheel,

$$\left.\begin{aligned} v_{2n} &= (v - \dot{\theta}_z l_2) \\ v_{2t} &= u \end{aligned}\right\} \tag{4.3}$$

From the Newton Euler equation,

$$\left.\begin{aligned} m\dot{u} &= m\dot{\theta}_z v + \sum F_x \\ m\dot{v} &= m\dot{\theta}_z u + \sum F_y \end{aligned}\right\} \tag{4.4}$$

where m is the vehicle mass, u is the longitudinal velocity, v is the lateral velocity, and $\dot{\theta}_z$ moment about z axis. F_{c1} and F_{c1} are the external forces, cornering forces F_{c1} and F_{c2} are the external force on front and rear wheel respectively in this bicycle vehicle model. δ is the steering angle in front wheel of bicycle vehicle model.

4.4 BOND GRAPH MODEL OF BICYCLE VEHICLE MODEL

The bond graph model shown in Fig. 4.2 is developed by above discussed kinematic relations. Electric motor gives power to rear wheel. The radius of rear wheel is r_r and front wheel radius is r_f . The distance between centre of gravity of vehicle and front wheel is l_1 and centre of gravity and rear wheel is l_2. The cornering forces are F_{c1} and F_{c2} on front and rear wheel respectively. The bond graph model of bicycle model is shown in Fig. 4.2.

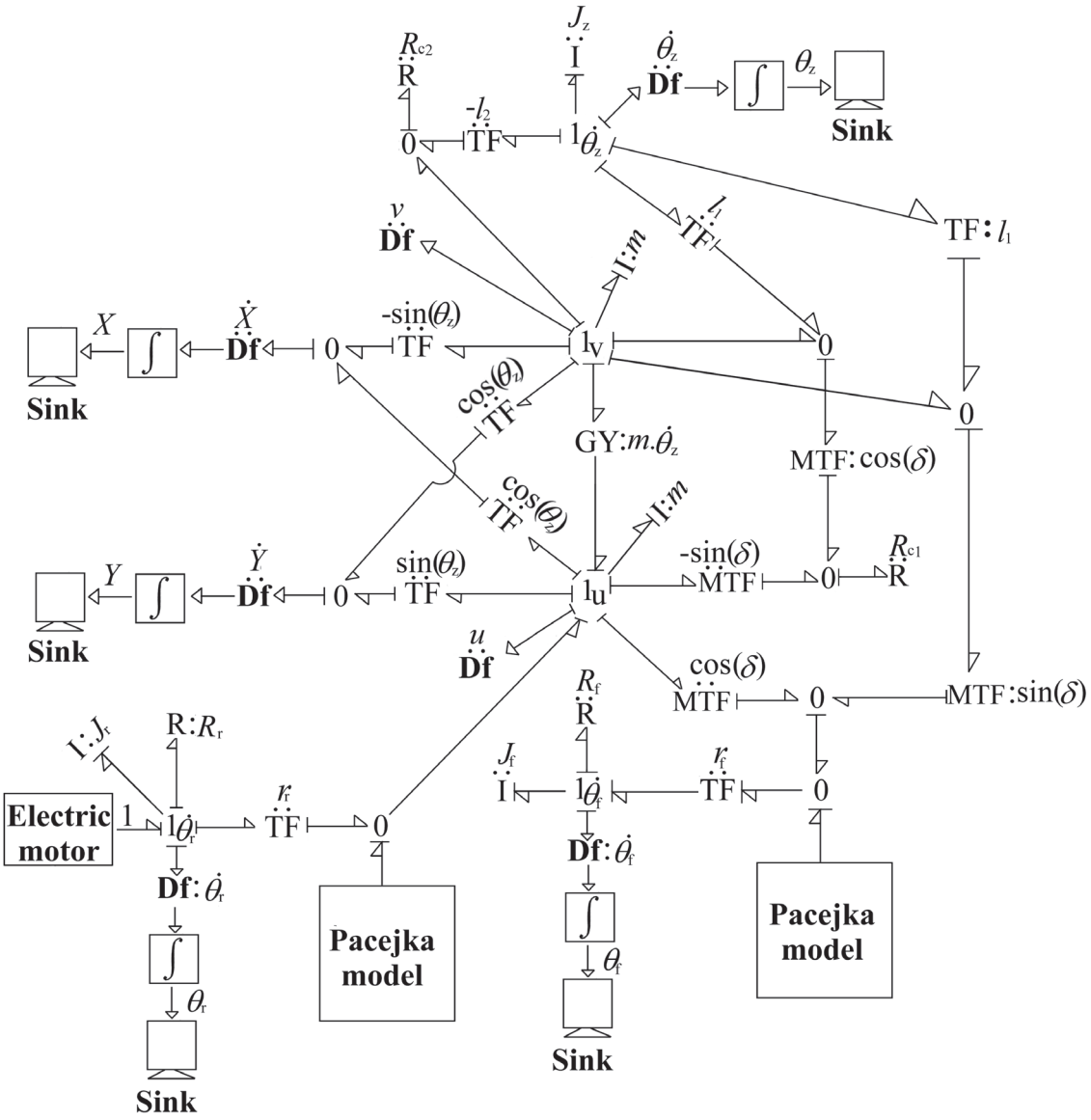

Fig. 4.2 Bond graph model of a bicycle vehicle model

In bicycle vehicle bond graph model, $(\mathrm{I}:m)$ is the bicycle vehicle mass and is $(\mathrm{I}:J_z)$ polar moment of inertia about z-axis. Flow detectors are attached at junctions 1_u , 1_v and $1_{\theta z}$

to measure the longitudinal, lateral and angular moment about z-axis respectively. Flow detector at zero junction measures the displacement in x and y directions with respect to inertial frame.

$$\left.\begin{aligned} \dot{X} &= u\cos\theta_z - v\sin\theta_z \\ Y &= u\sin\dot{\theta_z} + v\cos\theta_z \end{aligned}\right\} \tag{4.5}$$

The electric motor gives mechanical torque to the system. The rear wheel moment of inertia J_r returns flow as angular velocity of rear wheel. R_r is the tire damping coefficient in rear wheel. A flow detector is attached to measure the angular velocity $\dot{\theta}_r$ of rear wheel. This angular velocity transforms in linear velocity by transformer r_r. r_r is the rear wheel radius. Pacejka model gives the rolling resistance to the system. This rolling resisting force is depends on frictional coefficient μ and slip ratio.

Slip ratio for rear wheel,

$$SR_r = \frac{V_{rr} - u}{V_{rr}} \tag{4.6}$$

where V_{rr} $(r_r.\dot{\theta}_r)$ is the linear velocity of wheel in pure rolling condition and u is the longitudinal velocity of vehicle. Rolling resistance force in rear wheel,

$$Frr = D_{xr}.\sin(C_{xr}.a\tan(SR_r.B_{xr} + E_{xr}.(a\tan(SR_r.B_{xr}) - SR_r.B_{xr}))) \tag{4.7}$$

where B_{xr}, C_{xr}, D_{xr} and E_{xr} are the constant which depends on vehicle mass, tire and road surface conditions.

$$D_{xr} = \mu\frac{m.g}{2} \tag{4.8}$$

Rear wheel gives effort to vehicle CG. At the junction 1_u the inertial element vehicle mass m returns flow. This flow goes to front wheel and transformer $\cos(\delta)$ is multiplied with this flow. $(\dot{\theta}_z.l_1 + v)\sin\delta$ flow added with $u.\cos\delta$, this flow goes in front wheel. Cornering forces on front and rear wheel are modelled by resistive element R_{c1} and R_{c2} respectively.

$$effoert = flow \times R \tag{4.9}$$

R_{c1}, R_{c2} are the function of side slip angle in front and rear wheel. Slip angle is a ratio of transverse velocity and longitudinal velocity.

Side slip angle in front wheel,

$$X_f = \frac{v + \dot{\theta}_z l_1 \cos\delta - u\sin\delta}{v + \dot{\theta}_z l_1 \sin\delta + u\cos\delta} \tag{4.10}$$

Slip angle in rear wheel,

$$X_r = \frac{v - \dot{\theta}_z l_2}{u} \tag{4.11}$$

$$R_{c1} = \frac{D_{yf}\sin\left(C_{yf}a\tan\left(B_{yf}X_f - E_{yf}\left(B_{yf}X_f - a\tan\left(B_{yf}X_f\right)\right)\right)\right)}{v + \dot{\theta}_z l_1\cos\delta - u\sin\delta} \tag{4.12}$$

$$R_{c2} = \frac{D_{yr}\sin\left(C_{yr}a\tan\left(B_{yr}X_r - E_{yr}\left(B_{yr}X_r - a\tan\left(B_{yr}X_r\right)\right)\right)\right)}{v - \dot{\theta}_z l_2} \tag{4.13}$$

Rolling resistive force on front wheel is introduced by pacejka model. Rolling resistance force in front wheel,

$$F_{\mathrm{rf}} = D_{\mathrm{xf}}.\sin(C_{\mathrm{xf}}.a\tan(SR_{\mathrm{f}}.B_{\mathrm{xf}} + E_{\mathrm{xf}}.(a\tan(SR_{\mathrm{f}}.B_{\mathrm{xf}}) - SR_{\mathrm{f}}.B_{\mathrm{xf}}))) \tag{4.14}$$

where B_{xr}, C_{xr} , D_{xr} and E_{xr} are the constant which depends on vehicle mass, tire and road surface conditions.

$$D_{\mathrm{xf}} = \mu\frac{m.g}{2} \tag{4.15}$$

SR_{f} is the slip ratio in front wheel. In case of front wheel slip ratio will be different than rear wheel. Front wheel linear velocity will always less than the vehicle longitudinal velocity. Vehicle CG is pushing front wheel,

$$SR_{\mathrm{r}} = \frac{u - V_{\mathrm{rf}}}{u} \tag{4.16}$$

4.3 VEHICLE MODEL WITH MANUAL STEERING

In bond graph model of bicycle vehicle model Fig. 4.2 the value of modulated transformer MTF is modulated by steering angle δ. Bond graph model of manual steering is shown in Fig. 4.3. Steering angle δ is the output of bong graph model of manual steering.

$$Rack\,force = T_{\mathrm{c}} \times r_{\mathrm{g}} \tag{4.17}$$

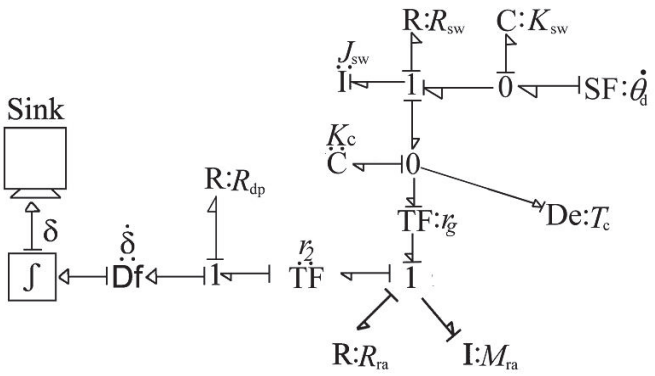

Fig. 4.3 Bond graph model of manual steering

In bond graph model of manual steering SF is a source of flow. K_{SW} is the stiffness of steering wheel. R_{sw} is damping coefficient of steering wheel, J_{sw} is the moment of inertia of steering wheel, K_c stiffness of steering column. R_{ra} is damping coefficient of Rack and pinion arrangement, M_{ra} is mass of rack. Damper R_{dp} prevent the fluctuation in the output of the system. Steering is applied at 25 second. The manual steering performance results are shown in Fig. 4.4 and Fig. 4.5. Simulation parameters are given in Table 4.1.

Table 4.1: Parameter values for bicycle vehicle model with manual steering

Steering Parameter			
Parameter	**Value**	**Parameter**	**Value**
J_{sw}	0.1 kg m^2	K_c	10^8 N/m
R_{sw}	0.01 N s/m	M_{ra}	20 kg
K_{SW}	10^6 N/m	R_{ra}	0.01 N s/m
r_g	0.1	R_{dp}	100 N s/m
r_2	0.02	$\dot{\theta}_d$	0.1 rad/s
Bicycle vehicle model Parameter			
Parameter	**Value**	**Parameter**	**Value**
m	1600 kg	E_{xf}	-2.0
J_z	100 kg m^2	B_{xf}	8.33
J_r	10 kg m^2	C_{xf}	1.2
J_f	10 kg m^2	E_{xf}	-2.0
r_f	0.3 m	B_{xf}	8.33

r_r	0.3 m	C_{xf}	1.2
l_1	1 m	E_{xf}	-2.0
l_2	1 m	B_{xf}	8.33
μ	0.78	C_{xf}	1.2
B_{xf}	8.33	E_{xf}	-2.0
C_{xf}	1.2		

4.3.1 Simulation result of bicycle vehicle model with manual steering

The bond graph model of inverse bicycle vehicle in connected with forward bicycle vehicle model by a overwhelming controller. Flow detector measures the angular velocities and longitudinal velocity in bond graph model.

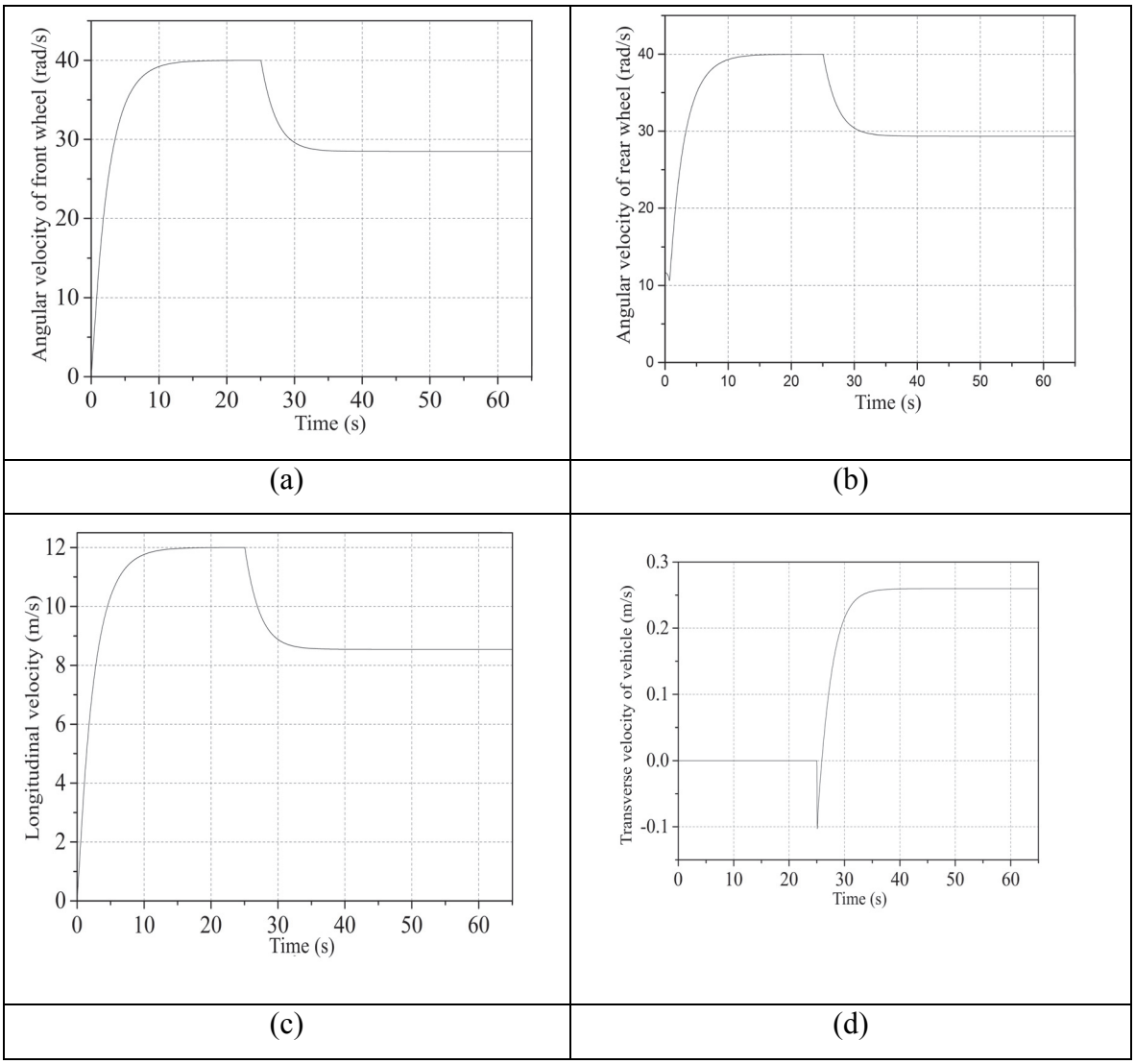

Fig. 4.4 (a) Angular velocity of front wheel, (b) Angular velocity of rear wheel, (c) Longitudinal velocity vehicle, (d) Transverse velocity vehicle

Simulation result shows that bicycle vehicle model start from zero velocity and accelerate after 12 second vehicle model get 12 m/s constant speed. Steering is applied at 25 second. These velocities are with respect to body fixed coordinate system. At 25 second steering is applied the vehicle GC moves toward steering direction while rear wheel were moving straight by which at 25 second transverse velocity is negative. The angular velocity of front and rear wheel is same and it validate by the relation,

$$v = r.\times\omega \tag{4.18}$$

where v is the longitudinal velocity of vehicle and ω is the angular velocity of wheel.

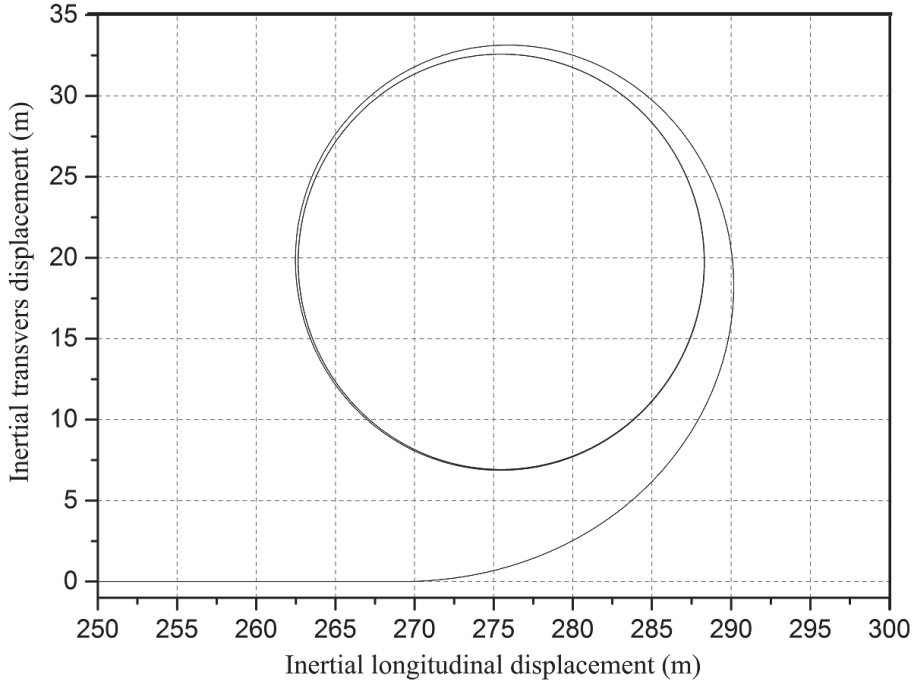

Fig. 4.5 Longitudinal vs transvers displacement in inertial frame manual steering

This plot shows the x y trace of vehicle GC in inertial coordinate frame. Steering is applied on a constant speed.

4.4 VEHICLE MODEL WITH ELECTRICAL POWER STEERING

As discussed in literature electrical power steering provides an assist torque by an electric motor. In this section EPS system is attached with vehicle bicycle model. The bond graph model of EPS is shown in Fig. 4.6.

In bond graph model of electrical power steering, an electrical motor is attached with steering rack by a ball screw. SE is a source of effort for electric motor. L_i is the coil

inductance and R_c is the coil resistance of assist motor. μ_{mo} is the motor constant. R_{sh} is the motor shaft damping coefficient. r_1 is ball screw reduction ratio. Other steering components are same as manual steering component. K_{SW} is the stiffness of steering wheel. R_{sw} is damping coefficient of steering wheel, J_{sw} is the moment of inertia of steering wheel, K_c stiffness of steering column. R_{ra} is damping coefficient of Rack and pinion arrangement, M_{ra} is mass of rack. Bicycle vehicle model and steering model parameter are same as previous. Assist motor, ball screw and motor shaft is attached with existing manual steering system. At junction 1

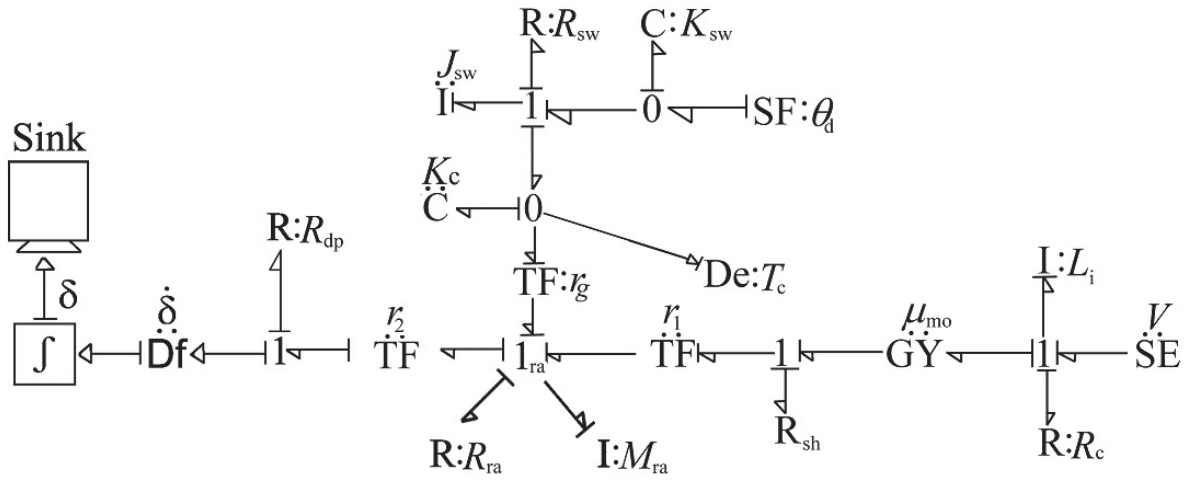

Fig. 4.6 Inverse steering bond graph model

The assist torque multiplied by transformer r_1, steering column torque multiplied with reduction gear ratio r_g .

$$Rack\ force = T_a \times r_1 + T_c \times r_g \tag{4.19}$$

where T_a is the assist torque and T_c is steering column torque

Table 4.2: Parameter values for EPS

EPS Parameter			
Parameter	**Value**	**Parameter**	**Value**
R_c	0.01 Ω	V	12 volt
μ_{mo}	0.1	R_{sh}	0.01 N s/m
r_1	0.5 m-1	L_i	10-2 H
J_{sw}	0.1 kg m2	K_c	108 N/m
R_{sw}	0.01 N s/m	M_{ra}	20 kg
K_{SW}	10^6 N/m	R_{ra}	0.01 N s/m
r_g	0.1 m^{-1}	R_{dp}	100 N s/m
r_2	0.02	$\dot{\theta}_d$	0.1 rad/s
Bicycle Vehicle Parameter			
Parameter	**Value**	**Parameter**	**Value**
m	1600 kg	E_{xf}	-2.0
J_z	100 kg m^2	B_{xf}	8.33
J_r	10 kg m^2	C_{xf}	1.2
J_f	10 kg m^2	E_{xf}	-2.0
r_f	0.3 m	B_{xf}	8.33
r_r	0.3 m	C_{xf}	1.2
l_1	1 m	E_{xf}	-2.0
l_2	1 m	B_{xf}	8.33
μ	0.78	C_{xf}	1.2
B_{xf}	8.33	E_{xf}	-2.0
C_{xf}	1.2		

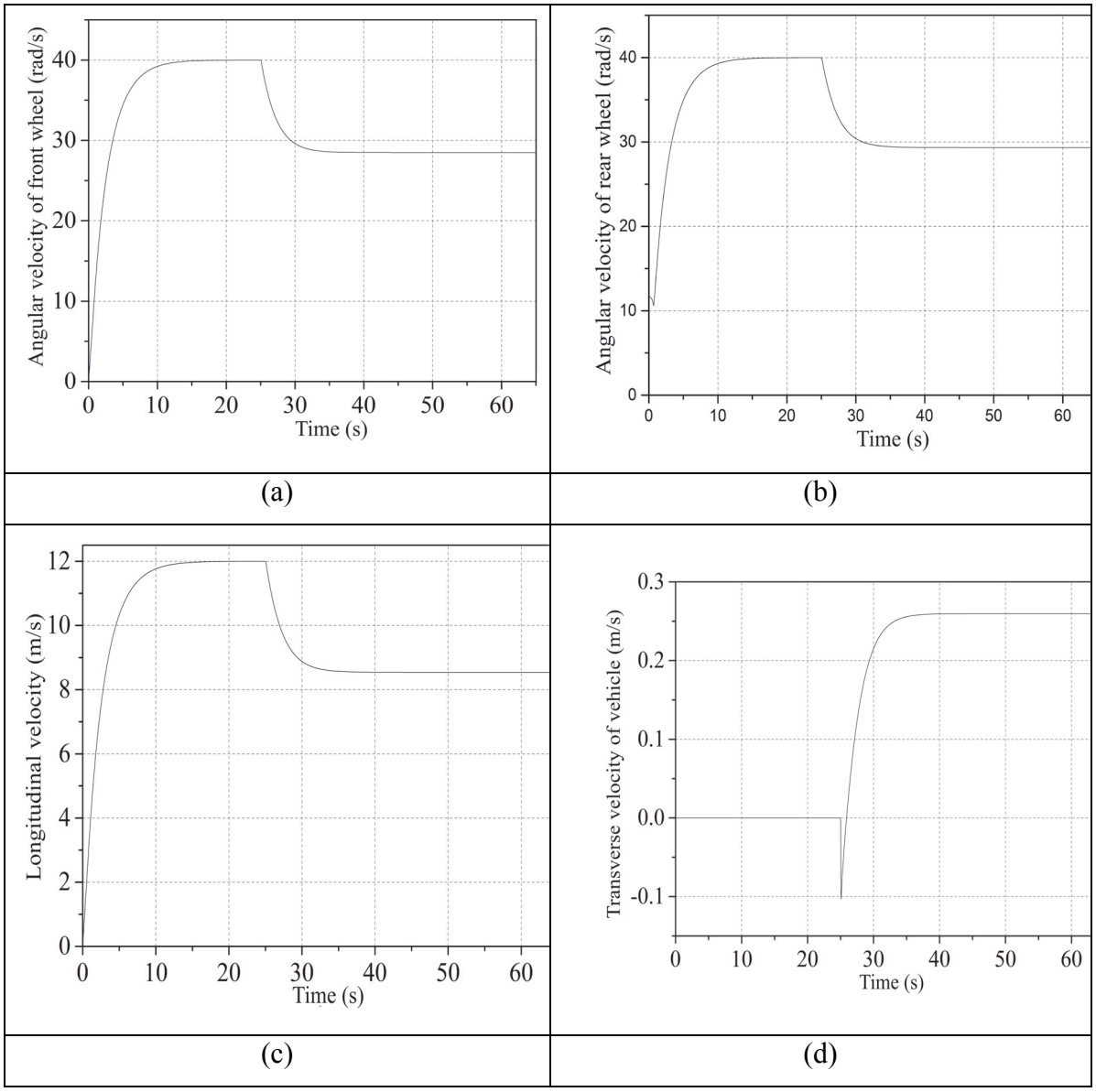

Fig. 4.7 (a) Angular velocity of front wheel, (b) Angular velocity of rear wheel, (c) Longitudinal velocity of centre of mass of vehicle, (d) Transverse velocity of centre of mass of vehicle

Figure 4.8 Longitudinal vs transvers displacement in inertial frame with EPS

The result shown that at same steering wheel movement, angular velocities of wheels, longitudinal velocity and transverse velocity are same. Comparing Fig. 4.5 and Fig 4.8 the radius of curvature is different *i.e.*, vehicle response is different. A comparative study of steering response is required.

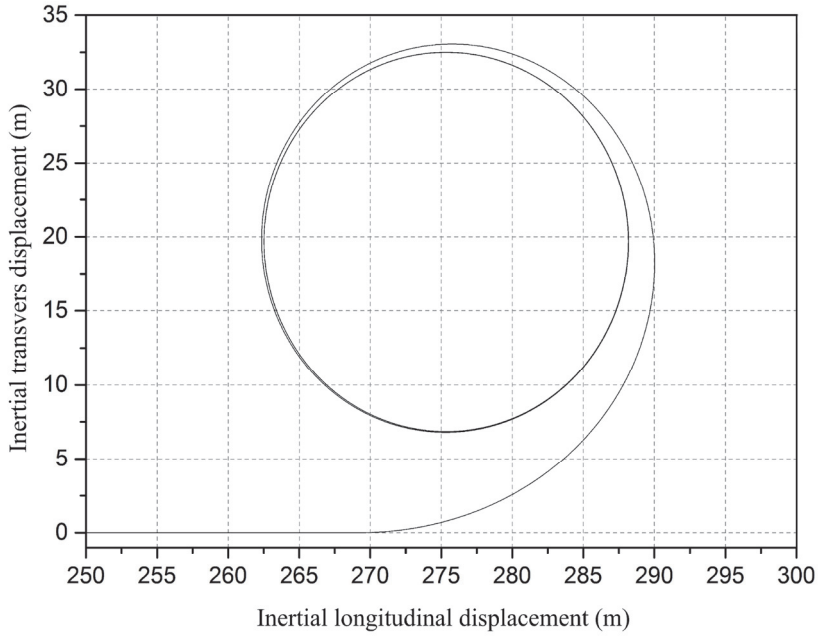

Fig. 4.8 Longitudinal vs transvers displacement in inertial frame with EPS

Steering angle 0.5 radian is applied from 25 second to 65 second. . The vehicle velocity is decreases and steering takes some response time. In starting cornering forces are not balanced with centripetal force of vehicle CG. After some second centripetal force is properly balanced with cornering forces and vehicle moves on a constant radius path.

4.5 COMPARATIVE PERFORMANCE ANALYSIS

A flow detector is attached in manual steering and electrical power steering for measuring the output. A graph is plotted for comparing between these detectors output. Fig. 4.9 shows this comparative study of manual steering with EPS.

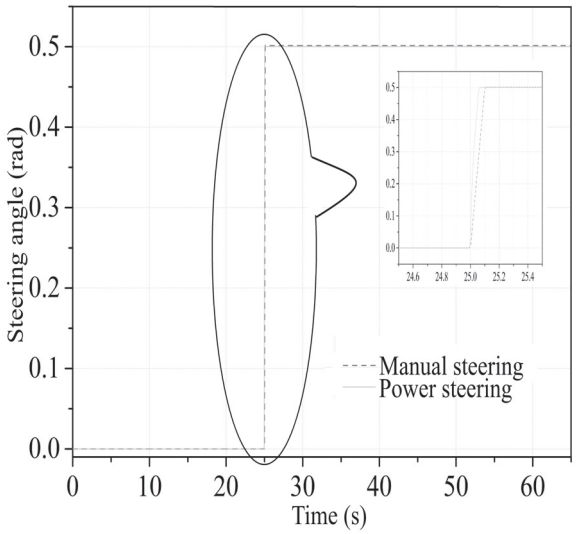

Fig. 4.9 Steering response in manual and Power steering

This is also observe that response is increases faster as the assist torque is increases. For developing an inverse vehicle dynamic bicycle vehicle model electrical power steering is very useful due to high response. Eqs. 4.12 and 4.14 show the rack force. In case of EPS rack force is more than manual steering since vehicle will easily steer in case of EPS.

CHAPTER 5: INVERSE VEHICLE MODEL OF BICYCLE

5.1 Introduction

This chapter introduces the inverse vehicle model, it is reasonable to give a trajectory and to make the vehicle tracking along it. A bond graph inverse dynamic model of bicycle model and inverse model of steering is developed. The input for the inverse model is x-y coordinate of the path. In bond graph model of inverse vehicle model three ghost controller and a forward bicycle model capsules are used. Results shows command trajectory and response trajectory.

5.2 Inverse Vehicle Model

An inverse vehicle model gives the required torque according to command trajectory. The command trajectory coordinates and vehicle orientation are in global coordinate system while steering angle will be in inertial coordinate. The derivative of global displacements gives the longitudinal and transverse velocities of vehicle with respect to global coordinate system. The velocities with respect to inertial frame are drawn by transformation matrix.

5.2.1 Kinematic Relation

The kinematic are used to make most of the part of inverse model. It is assumed that longitudinal and transverse velocity of vehicle are u and v respectively and steering angle is very small and slip in longitudinal and transverse direction is negligible.

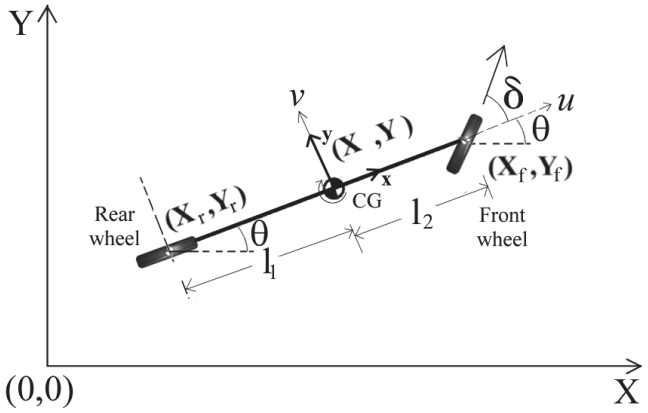

Fig. 5.1 Bicycle vehicle model with global coordinate

In Fig. 5.1 bicycle vehicle model is shown, steering angle is δ. $(X_{f,}Y_f)$, $(X_{r,}Y_r)$ and $(X_{,}Y)$ are the co-ordinates of front wheel, rear wheel and center of gravity of vehicle with respect to inertial frame. A local coordinate system which is attached with CG of bicycle vehicle and X-Y is the global coordinate system. u and v are the vehicle velocity in body

fixed coordinate frame. $\dot{X}$ And $\dot{Y}$ is the velocity of vehicle with respect to global coordinate system.

$$\begin{bmatrix} \dot{X} \\ \dot{Y} \end{bmatrix} = \begin{bmatrix} \cos(\theta) & -\sin(\theta) \\ \sin(\theta) & \cos(\theta) \end{bmatrix} \begin{bmatrix} u \\ v \end{bmatrix} \tag{5.1}$$

Since,

$$\begin{bmatrix} u \\ v \end{bmatrix} = \begin{bmatrix} \cos(\theta) & -\sin(\theta) \\ \sin(\theta) & \cos(\theta) \end{bmatrix}^{-1} \begin{bmatrix} \dot{X} \\ \dot{Y} \end{bmatrix} \tag{5.2}$$

$$\dot{X}_{\mathrm{f}} \sin(\theta+\delta) - \dot{Y}_{\mathrm{f}} \cos(\theta+\delta) = 0 \tag{5.3}$$

$$\dot{X}_{\mathrm{r}} \sin(\theta) - \dot{Y}_{\mathrm{r}} \cos(\theta) = 0 \tag{5.4}$$

$$X_f = X_r + (l_1 + l_2)\cos(\theta) \tag{5.5}$$

$$Y_f = Y_r + (l_1 + l_2)\sin(\theta) \tag{5.6}$$

By Eqs. (5.1) and (5.2),

$$\frac{d}{dt}(X_r + (l_1+l_2)\cos(\theta))\sin(\theta+\delta) - \frac{d}{dt}(Y_r + (l_1+l_2)\sin(\theta))\cos(\theta+\delta) = 0$$

$$\Rightarrow \dot{X}_r \sin(\theta+\delta) - \dot{Y}_r \cos(\theta+\delta) - \dot{\theta}(l_1+l_2)(\sin(\theta)\sin(\theta+\delta) - \cos(\theta)\cos(\theta+\delta)) = 0$$

$$\Rightarrow \dot{X}_r \sin(\theta+\delta) - \dot{Y}_r \cos(\theta+\delta) - \dot{\theta}(l_1+l_2)\cos(\delta) = 0$$

Putting $\dot{X}_r = u\cos(\theta)$ & $\dot{Y}_r = u\sin(\theta)$ from Fig. 5.1

$$\Rightarrow u\cos(\theta)\sin(\theta+\delta) - u\sin(\theta)\cos(\theta+\delta) - \dot{\theta}(l_1+l_2)\cos(\delta) = 0$$

$$\Rightarrow u(\cos(\theta)\sin(\theta+\delta) - \sin(\theta)\cos(\theta+\delta)) - \dot{\theta}(l_1+l_2)\cos(\delta) = 0$$

$$\Rightarrow u\sin(\delta) - \dot{\theta}(l_1+l_2)\cos(\delta) = 0$$

$$\Rightarrow \frac{\sin(\delta)}{\cos(\delta)} = \frac{\dot{\theta}}{u}(l_1+l_2)$$

$$\Rightarrow \delta = a\tan\left((l_1+l_2)\frac{\dot{\theta}}{u}\right) \tag{5.7}$$

Since the Ackermann steering angle δ can therefore be expressed as an expiration of the longitudinal velocity u and yaw velocity $\dot{\theta}$ of the bicycle model of vehicle.

5.2.2 Bond graph Model

The inverse bond graph model of a bicycle vehicle model is drawn in Fig 5.2, Path co-ordinates X , Y and orientation of vehicle θ_{i} (input to inverse model) are shown by $\mathrm{MSf}:X$, $\mathrm{MSf}:Y$ and $\mathrm{MSf}:\theta_{\mathrm{i}}$ respectively. $I:J_{\mathrm{i}}$ is the virtual polar moment of inertial of inverse vehicle model about Z-axis, $I:m_{\mathrm{i}}$ is the virtual mass of inverse vehicle model. $\mathrm{I}:J_{\mathrm{ri}}$ and $\mathrm{I}:J_{\mathrm{fi}}$ are the polar moment of inertia of rear and front wheel respectively. GC is ghost control it takes input flow and gives effort output. $M_{\mathrm{C}}, k_{\mathrm{C}}, R_{\mathrm{C}}$ are the ghost controller virtual inertia, stiffness and damping coefficient respectively and R_{P} , k_{P} are the pad damping and pad stiffness to avoid the differential causality. The flow sensor Df is connected that gives the flow and displacement value at that junction. $\mathrm{TF}:r_{\mathrm{fi}}$, $\mathrm{TF}:r_{\mathrm{ri}}$ are rear and front wheels radius.

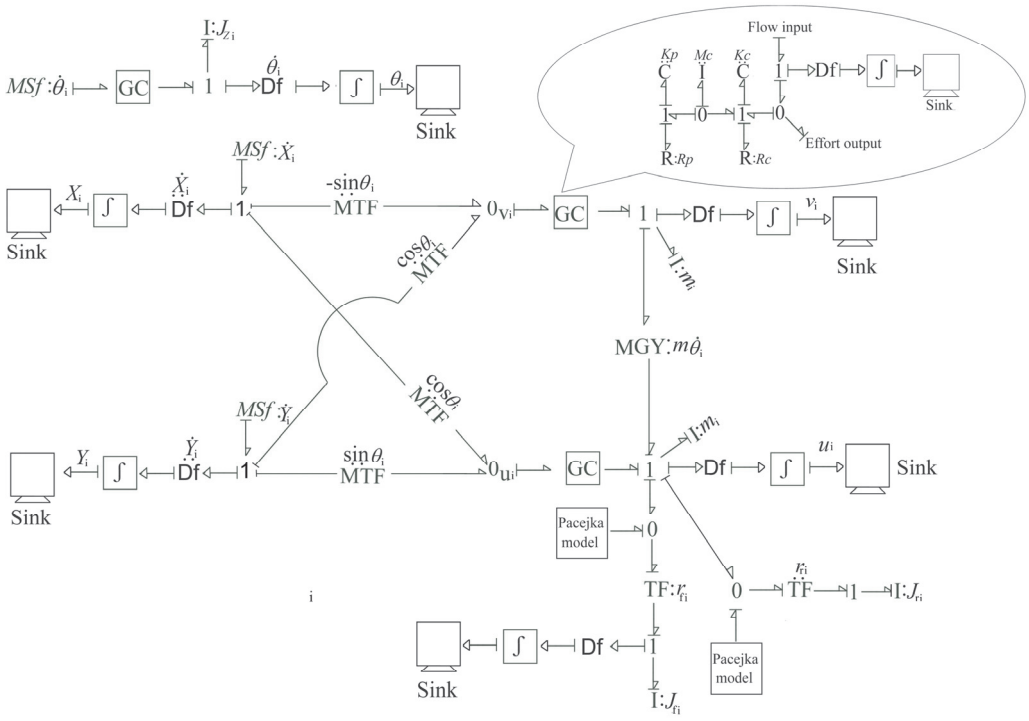

Fig. 5.2 Bond graph model of inverse bicycle vehicle model

Modulated gyrator ($MGY:m_{\mathrm{i}}.\dot{\theta}_{\mathrm{i}}$) is used to apply pseudo force in inverse model. Pacejka model gives the rolling resistance (F_{rri}) by the pacejka magic formula which gives the rolling resistance force. Rolling resistance force in rear wheel,

$$F_{\mathrm{rri}} = D_{\mathrm{xri}}.\sin(C_{\mathrm{xri}}.a\tan(SR_{\mathrm{ri}}.B_{\mathrm{xri}} + E_{\mathrm{xri}}.(a\tan(SR_{\mathrm{ri}}.B_{\mathrm{xri}}) - SR_{\mathrm{ri}}.B_{\mathrm{xri}}))) \tag{5.8}$$

$$SR_{\mathrm{ri}} = \frac{u_{\mathrm{i}} - v_{\mathrm{rri}}}{u_{\mathrm{i}}} \tag{5.9}$$

Rolling resistance force in front wheel,

$$F_{\mathrm{rfi}} = D_{\mathrm{xfi}}.\sin(C_{\mathrm{xfi}}.a\tan(SR_{\mathrm{fi}}.B_{\mathrm{xfi}} + E_{\mathrm{xfi}}.(a\tan(SR_{\mathrm{fi}}.B_{\mathrm{xfi}}) - SR_{\mathrm{fi}}.B_{\mathrm{xfi}}))) \tag{5.10}$$

$$SR_{\mathrm{fi}} = \frac{u_i - v_{\mathrm{rfi}}}{u_i} \tag{5.11}$$

In inverse model the effort is applied by ghost controller on GC of inverse vehicle. Inverse vehicle CG will push the front wheel and pull the rear wheel.

where $B_{\mathrm{xf}i}$, $C_{\mathrm{xf}i}$, $E_{\mathrm{xf}i}$, $B_{\mathrm{xr}i}$, $C_{\mathrm{xr}i}$, and $E_{\mathrm{xr}i}$ are the constant which depends on vehicle mass, tire and road surface conditions.

$$D_{\mathrm{xr}i} = \mu_i \frac{m_i.g}{2} \tag{5.12}$$

$$D_{\mathrm{xfi}} = \mu_i \frac{m_i.g}{2} \tag{5.13}$$

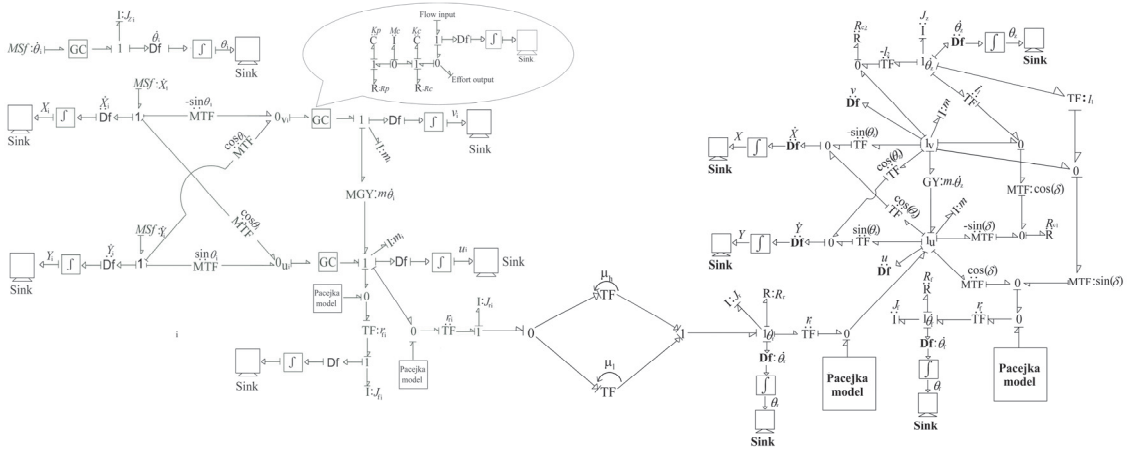

Fig. 5.3 Inverse bicycle vehicle model with forward model

The inverse bicycle vehicle model is connected with forward model by overwhelming controller as shown in Fig. 5.3. The inverse bond graph model of steering Fig. 5.4 is a mirror image of forward steering bond graph model that has been discussed in chapter 4. The ghost controller CG is similar as discussed in inverse vehicle bond graph model. Steering angle δ input of inverse steering model is calculated by equation (5.7). $GY:\mu_{mo}$ and $\mathrm{I}:L_{\mathrm{i}}$ are motor parameter motor constant Coil resistance and inductance respectively. $\mathrm{R}:R_{\mathrm{sh}}$, $\mathrm{R}:R_{\mathrm{ra}}$ are damping coefficient of motor shaft and rack, $\mathrm{I}:M_{\mathrm{ra}}$ is rack mass. Inverse model of steering gives the voltage output. This voltage goes into forward model of steering.

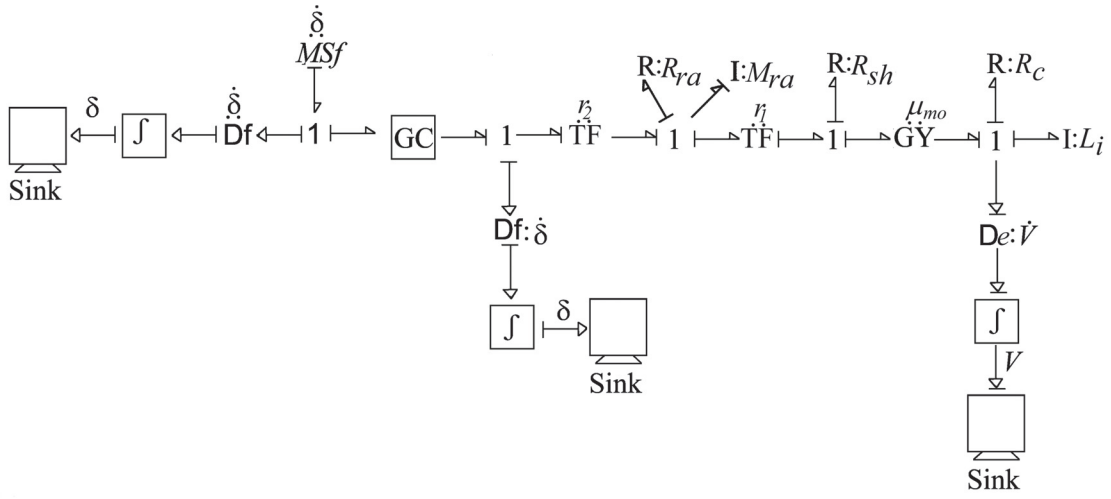

Fig. 5.4 Bond graph model of inverse steering model

System differential equation generates by system bond graph model. System differential equation solved by computer. Bond graph simulation is done on SYMBOL SHAKTI software.

5.3 Parameter values and simulation results:

Bond graph model is used to generate system differential equations. These equations are solved by computer. This thesis SYMBOL SHAKTI software is used to solve the system equations.

Table:5.1 Inverse bicycle vehicle model, Inverse steering, ghost controller, over whelming controller and forward bicycle vehicle model parameter

Inverse Bicycle Vehicle Bond Graph Model Parameter			
Parameter	Value	Parameter	Value
m_i	1000 kg	E_{xfi}	-2.0
J_{zi}	100 kg m^2	B_{xfi}	8.33
J_{ri}	10 kg m^2	C_{xfi}	1.2
J_{fi}	10 kg m^2	E_{xfi}	-2.0
r_{fi}	0.3 m	B_{xfi}	8.33
r_{ri}	0.3 m	C_{xfi}	1.2
l_{1i}	1 m	E_{xfi}	-2.0
l_{2i}	1 m	B_{xfi}	8.33
μ_i	0.8	C_{xfi}	1.2
B_{xfi}	8.33	E_{xfi}	-2.0
C_{xfi}	1.3		

Inverse Steering Bond Graph Model Parameter			
Parameter	Value	Parameter	Value
J_{swi}	0.1 kg m^2	K_{ci}	10^8 N/m
R_{swi}	0.01 N s/m	M_{rai}	20 kg
K_{SWi}	10^6 N/m	R_{rai}	0.01 N s/m
r_{gi}	0.1	R_{dpi}	100 N s/m
r_{2i}	0.02		
Ghost Controller Parameter			
Parameter	Value	Parameter	Value
k_c	10^{10} N/m	R_c	10^4 N s/m
k_p	10^{12} N/m	M_c	10 kg
R_p	10^6 N s/m		
Overwhelming Controller Parameter			
Parameter	Value	Parameter	Value
μ_h	100	μ_l	1
Forward Bicycle Bond Graph Model Parameter			
Parameter	Value	Parameter	Value
m	1600 kg	E_{xf}	-2.0
J_z	100 kg m^2	B_{xf}	8.33
J_r	10 kg m^2	C_{xf}	1.2
J_f	10 kg m^2	E_{xf}	-2.0
r_f	0.3 m	B_{xf}	8.33
r_r	0.3 m	C_{xf}	1.2
l_1	1 m	E_{xf}	-2.0
l_2	1 m	B_{xf}	8.33
μ	0.78	C_{xf}	1.2
B_{xf}	8.33	E_{xf}	-2.0
C_{xf}	1.4		
Steering Bond Graph Model Parameter			
Parameter	Value	Parameter	Value
r_g	0.1	R_{dp}	100 N s/m
r_2	0.02	$\dot{\theta}_d$	0.1 rad/s
J_{sw}	0.1 kg m^2	K_c	10^8 N/m
R_{sw}	0.01 N s/m	M_{ra}	20 kg
K_{SW}	10^6 N/m	R_{ra}	0.01 N s/m

A straight path coordinate are given to inverse model and simulate 25 second. The angular velocity of rear wheel, angular velocity of front wheel and velocity of vehicle in controller model and forward model are shown in Fig. 5.4 and Fig. 5.5.

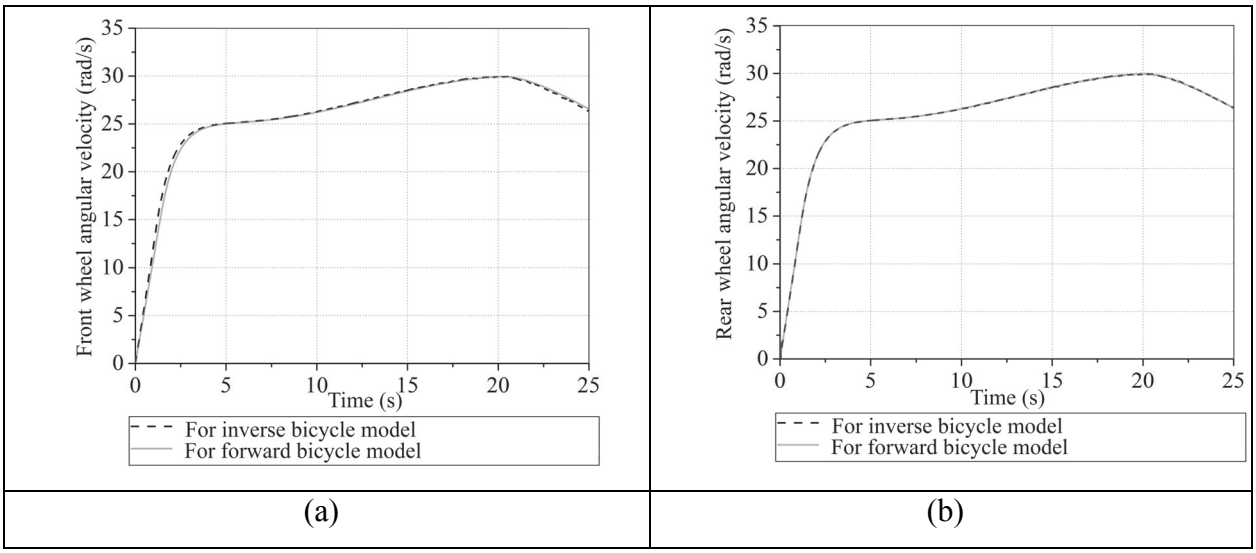

Fig. 5.5 (a) Front wheel angular velocity (b) Rear wheel angular velocity

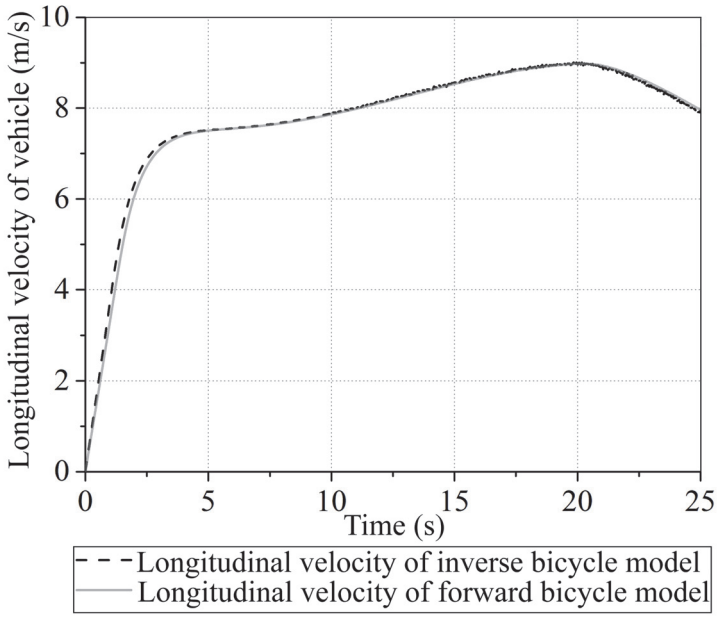

Fig. 5.6 Longitudinal velocity

In this simulation forward vehicle moves on a straight path, accelerate till 5 second then decelerate and again accelerate up to 20 second and then decelerate and tracks a path. Inverse vehicle model which is a virtual vehicle computes longitudinal velocity, angular velocities of wheels. Inverse vehicle model gives rear wheel torque for forward vehicle model. The forward bicycle vehicle model velocities as same as inverse model. Wheels

angular velocities plots with time are shown in Fig. 5.5(a),(b). the angular velocities are same in inverse model and forward model.

5.3.1 Trajectory tracking of vehicle with no steering

In this simulation inverse vehicle model with forward vehicle model is tested for high acceleration and deceleration conditions. Inverse model gives required toque for forward model.

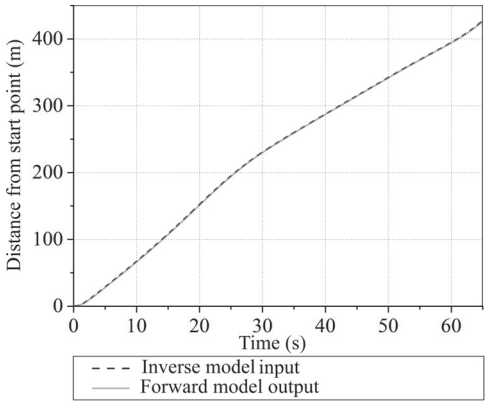

Fig. 5.7 Input and output path vs time

Simulation for acceleration deceleration is done for 65 second. In Fig. 5.7, the stating time zero to 25 second slope of the graph is more than the 25 to 65 second. Vehicle is accelerate till 25 second then decelerate. Input distance in inverse vehicle model and output from the forward model is same. Inverse vehicle model with forward bicycle model is performing is good enough in case of high acceleration and deceleration.

5.3.2 Trajectory tracking of vehicle with steering

The steering angle is computed by eqn. 5.7, the vehicle longitudinal velocity and yaw rate is detected by flow detector as shown in Fig. 5.2.The value of steering angle is a input in modulated transformer in forward model. The required rear wheel torque is applied by inverse vehicle model and steering angle is computed by algorithm to track the input path.

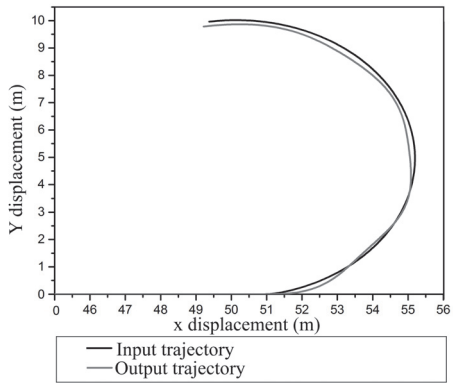

Fig. 5.8 Trajectory tracking with stearing

In Fig. 5.8 the input and output trajectory are shown, X axis of graph is showing displacement of vehicle CG in X asis direction and Y axis showing displacement in Y direction. These values are in global coordinate system. Due to side slip angle which is highly nonlinear, there is very minute error. Vehicle is successfully take a U-turn.

CHAPTER: 6 CONCLUSION

6.1 CONCLUSION

The main objective of this thesis was to develop an inverse vehicle dynamic controller which gives the required torque to get a predefined kinematic response of a bicycle vehicle.

Bond graph modelling of electrical power steering and bond graph modelling of vehicle is considered in chapret2. Bond graph modelling of multi body system and bond graph modelling of vehicle are considered in chapter 3. In chapter 4 by bond graph modelling a comparative study of electrical power steering and manual steering with bond graph model of bicycle vehicle is done. The response of electrical power steering is faster than manual steering.

In chapter ghost controller, overwhelming controller and bicycle vehicle inverse model simulation shows the performance. Overwhelming controller is able to solve the robustness problem of forward model.

6.2 FUTURE SCOPE

Based on this thesis the following area of work are suggested for future exploration.

- This work can extended to develop autonomous four wheel vehicle model to trajectory tracking.
- Electrical system may be used in four wheel vehicle body to get better steering response
- This thesis is limited to small steering angle and low velocity of vehicle because at large steering angle there is side slip which effect the vehicle steering. In case of large side slip, vehicle does not follow Ackermann steering condition.

REFERENCES

1. Toroyan, T., The Global status report on road safety 2013, World health organization, Geneva, 2013.
2. Siciliano, B., Khatib O., Intelligent vehicles In: Springer handbook of robotics, 2008, p.1191.
3. Sharkey, N., The programmable robot of ancient Greece, New Scientist Magazine Issue 2611, 4th July 2007.
4. Dickmanns, E, Zapp ,A., Autonomous High Speed Road Vehicle Guidance by Computer Vision. In: Triennial World Congress of the International Federation of Automatic Control, Volume IV, July 1987.
5. Pomerleau, D., An Autonomous Land Vehicle in a Neural Network. In: Advances in Neural Information Processing Systems, Morgan Kaufmann, San Mateo, CA (1989).
6. Shin'ichi, Y., Control of Vehicle with Power Wheeled Steering Using Feed Forward Dynamics Compensation IEEE, 1991.
7. Thrun, S., Montemerlo, M., Dahlkamp, H., The Robot That Won the DARPA Grand Challenge. Journal of Field Robotics 23(9), 661–692 (2006).
8. Ferries, G., Control/Structure Interaction in Hydraulic Power Steering Systems, Society of Automotive Engineers, American control conference, June 1997.
9. Tanaka, T., Daikoku, A., Imagi, A., Yoshikua,Y., An Advanced Electrical Power Steering Motor , Society of Automotive Engineers, 2001.
10. Akhataruzzaman, Md., Norrul, A., Razali, M., An Experiment on Electric Power Steering (EPS) System of a Car, IEEE, Applied mechanics and materials, 2012
11. Guobiao1, S., Zhao, S., Simulation Analysis for Electric Power Steering Control System Based On Permanent Magnetism Synchronization Motor, ,2nd International Conference on Electronic & Mechanical Engineering and Information Technology, Jun 2012.
12. Pacejka H.B., Tyre and Vehicle Dynamics, Butterworth-Heinemann, 2006

13. Merzouki, R., Ould-Bouamama, B., Djeziri, M. A., and Bouteldja, M. Modelling and estimation of tire–road longitudinal impact efforts using bond graph approach. Mechatronics, 2007a, 17 (2–3), 93–108.
14. Gawthrop, P. J., Jones, R. W., and Mackenzie, S. A. Identification of partially-known systems. Automatica , 1992, 28 (4), 831–836.
15. Merzouki, R., Medjaher, K., Djeziri, M. A., and Ould-Bouamama, B. Backlash fault detection in mechatronic system. Mechatronics , 2007b, 17 (6), 299–310
16. Ould Bouamama, B., Medjaher, K., Samantaray, A. K., and Staroswiecki, M. Supervision of an industrial steam generator. Part I: Bond graph modelling. Control Engineering Practice , 2006, 14 (1), 71–83.
17. Ould Bouamama, B., Medjaher, K., Bayart, M., Samantaray, A. K., and Conrard, B.Fault detection and isolation of smart actuators using bond graphs and external models. Control Engineering Practice , 2005, 13 (2), 159–175.
18. Silva Luis I., Magallan Guillermoa, Angelo Cristian H. De, Garcia Guillermo O., Vehicle Dynamics Using Multi Bobd Graphs Four Wheel Electric Vehicle Modeling, IEEE, 2008.
19. Karnopp, D.C., Margolis, D.L., Rosenberg R.C., System Dynamics: Modeling and Simulation of Mechatronic Systems, Wiley, New York, 2000.
20. Margolis D., Shim Taehyun, A bond graph model incorporating sensors, actuators, and vehicle dynamics for developing controllers for vehicle safety, Journal of The Franklin Institute, 338, 2001, 21-34
21. Rucco A., Notrro, G., Haeser, J., Dynamics exploration of a Car Model with Load Transfer, Dicision and Control, IEEE, Dec 2010, 15-17.
22. Karnopp, D. C., Margolis, D. L., and Rosenberg, R. C. System Dynamics, Modelling and Simulation of Mechatronic Systems, 2000 (John Wiley & Sons,NY).
23. Bos, A., M., Modelling Multibody Systems in terms of Multibond Graphs, with application to a motorcycle, PhD thesis at Twente University, 1986
24. McCann, R.,Variable Effort Steering for Vehicle Stability Enhancement Using an Electric Power Steering System , SAE 2000.
25. Yu H., Liang, W., Kuang M., MeGee, R., Vehicle Handling Assistant Control System via Independent Rear Axle Torque Biasing, American Control Conference, 2009.

26. Gillies G.J., Human factors assessment of vehicle power steering, Ergonomics, 26 April 2007
27. Badawy A., Bolourchi F., Gaut S., Modelling and analysis of Electric Power Steering, SAE, 1999.
28. Gillies G.J., Human factors assessment of vehicle power steering, Ergonomics, IEEE, 26April2007.
29. Garcia-Gomez J., Dauphin T. G., Rombaut Ch., Average Bond Graph Models of DC Power Converters, International Conference on Bond Graph Modeling and Simulation, volume 31(1) of Simulation Series, 1999, 338–343
30. Badawy, A., Bolourchi, F., Gaut, S., Modelling and analysis of Electric Power Steering, SAE, 1999.
31. Zang, H., Liu, M., Automation and Logistics, IEEE International Conference, Aug. 2007.
32. Yaohua H., Can Y., Fangfang, L., Study of Linear Electric Power Steering System, IEEE, 2011.
33. Jerems, F., Proft, M., Rachui D., and Kalinin, V., A New Generation Nontorsion Bar Torque Sensors For Electromechanical Power Steereing Applications, Proc. Int. Congress on Electronic Systems for Vehicles, September, 2001, 27-28.
34. Stetter, R., Paczynski A., Intelligent Steering System for Electrical Power Train, Nov 2010,1-6.
35. Yuta, s., Shigeki, T., Control Of Vehicle With Power Wheeled Steering Using Feed Forward Dynamic Compensation, IEEE, 1991, 2264-2269.
36. Parmar, M., Hung, Y., A Sensor Less Optimal Control System For An Automotive EPS System, Volume 51,IEEE, 2 April/ 2004
37. Morton, C., Pickert, V., Self Alignment Torque as a Source of Energy Recovery for Hybrid Electric Trucks, Vol 63, IEEE, 2014.
38. Wang, Y., Wang, H., Development of steering simulator system for evaluation of Electrical Power Steering, IEEE, 2009, 1832-1836.
39. Qiang, L., Ren, H., Modeling and Simulation Study of The Steer Wire System Using Bong Graph, Vehicle Electronics and Safety, IEEE, 2005, 7-11.
40. Li, Q., Liang, X., Modeling and Simulation Study of The Steer Wire System Using Bong Graph, IEEE, April, 2010, 744-747.

41. Gawthrop, P.J., Beva, G.,P., Bond graph modelling, IEEE Control System Magzine, April, 2007, 25-45.

CURRICULUM VITAE

Anshuman did his graduation from Dr. K. N. Modi Institute, Modinagar in Bachelor of Mechanical Engineering (B. Tech), in the year 2010. After that he has worked as Graduate Engineer Trainee in Grip Engineers (P) Ltd., Faridabad, Hariyana, in the year 2010-2011 and As an Assistant design engineer in Telecom Network Solution (P) Ltd. NOIDA in the year 2011–2012. In the year 2012, he joined in the Master of Engineering (CAD/CAM Engineering) Programme at Thapar University, Patiala, Punjab. His ME thesis work is in the area of **Inverse Vehicle Dynamic Model of a Bicycle Vehicle with Power Steering**: **A Bond Graph Approach**.